International Journal of Bifurcation and Chaos, Vol. 22, No. 3 (2012) 1250068 (30 pages)

DOI: 10.1142/S021812741250068X

PERIOD ADDING IN PIECEWISE LINEAR MAPS WITH TWO DISCONTINUITIES

FABIO TRAMONTANA
Department of Economics and Quantitative Methods, University of Pavia, Italy
fabio.tramontana@unipv.it

LAURA GARDINI
Department of Economics, Society and Politics, University of Urbino, Italy
laura.gardini@uniurb.it

VIKTOR AVRUTIN* and MICHAEL SCHANZ†
Institute of Parallel and Distributed Systems, University of Stuttgart, Germany
**Viktor.Avrutin@ipvs.uni-stuttgart.de*
†*Michael.Schanz@informatik.uni-stuttgart.de*

Received January 31, 2011; Revised June 19, 2011

In this work we consider the border collision bifurcations occurring in a one-dimensional piecewise linear map with two discontinuity points. The map, motivated by an economic application, is written in a generic form and considered in the stable regime, with all slopes between zero and one. We prove that the period adding structures occur in maps with more than one discontinuity points and that the Leonov's method to calculate the bifurcation curves forming these structures is applicable also in this case. We demonstrate the existence of particular codimension-2 bifurcation (big-bang bifurcation) points in the parameter space, from which infinitely many bifurcation curves are issuing associated with cycles involving several partitions. We describe how the bifurcation structure of a map with one discontinuity is modified by the introduction of a second discontinuity point, which causes orbits to appear located on three partitions and organized again in a period-adding structure. We also describe particular codimension-2 bifurcation points which represent limit sets of doubly infinite sequences of bifurcation curves and appear due to the existence of two discontinuities.

Keywords: Piecewise linear discontinuous maps; period adding bifurcation structure; Leonov's approach; two discontinuity points.

1. Introduction

Since the pioneering works by Richard Day focused on piecewise linear maps (see e.g. [Day, 1982, 1994]), several applications to economics ultimately lead to models which are described by piecewise linear or piecewise smooth maps [Hommes, 1991, 1995; Hommes & Nusse, 1991; Hommes *et al.*, 1995; Gallegati *et al.*, 2003; Puu & Sushko, 2002, 2006; Sushko *et al.*, 2003, 2005, 2006; Gardini *et al.*, 2006a, 2006b, 2008]. In particular, several systems are modeled via *discontinuous maps*, often with *several discontinuity points* [Puu *et al.*, 2002, 2005; Puu, 2007; Sushko *et al.*, 2004; Tramontana *et al.*, 2009; Gardini *et al.*, 2011]. However, the bifurcations occurring in discontinuous models with more than two partitions have not yet been investigated. In this

work we start this subject, limiting our analysis to piecewise linear maps with two discontinuity points and positive slopes. We are motivated by the model introduced in [Tramontana *et al.*, 2009], where it is shown that a duopoly may give rise to discontinuous reaction functions, whose explicit formulation cannot be obtained. Observing, however, that the reaction functions are very flat, we have roughly (but quite realistically) approximated the pieces appearing in the reaction functions by pieces of straight lines, so formulating the following map T:

$$x' = T(x),$$
$$T(x) = \begin{cases} f_L(x) = a_L x + \mu_L & \text{if } x < d_1 \\ f_M(x) = a_M x + \mu_M & \text{if } d_1 < x < d_2 \\ f_R(x) = a_R x + \mu_R & \text{if } x > d_2 \end{cases} \tag{1}$$

and the slopes which are observed in the economic application are positive and smaller than 1, we shall assume

$$a_L,\ a_M,\ a_R \in (0,1), \quad d_1 < d_2. \tag{2}$$

In particular, an interesting example in the applied context is obtained by the following values:

$$\begin{gathered} a_L = 0.9, \quad a_M = 0.3, \quad a_R = 0.4, \\ \mu_L = 1, \quad \mu_M = 0.2 \end{gathered} \tag{3}$$

that we shall use in almost all the figures, to illustrate our results, which are however generic (for the case with slopes $a_i \in (0,1), i = L, M, R$), as the border collision bifurcation curves are given as a function of all the parameters of the map T. A qualitative example is shown in Fig. 1(a).

We also notice that we use the term "bifurcation curves" in a wider meaning, as we ought to call them, more properly, "bifurcation subspaces" in the whole parameter space. However, as we mainly show sections in a two-dimensional parameter space, fixing all the other parameters, for simplicity, we use everywhere the term bifurcation curves.

We are interested in the analysis of the bifurcations occurring as the discontinuity point d_1 increases, reaching the second discontinuity point d_2, after which the piece in the middle disappears and the map reduces to a map with only one discontinuity point [as shown in Fig. 1(b)], which we denote as map F:

$$x' = F(x),$$
$$F(x) = \begin{cases} f_L(x) = a_L x + \mu_L & \text{if } x < d_2 \\ f_R(x) = a_R x + \mu_R & \text{if } x > d_2. \end{cases} \tag{4}$$

Or, equivalently, starting from the model with only one discontinuity, $x' = F(x)$, we are interested in the bifurcations introduced by adding a second discontinuity point $d_1 < d_2$ starting from $d_1 = d_2$ and then decreasing d_1 in the map $x' = T(x)$. We shall follow this approach in the description of the bifurcation curves.

It is immediate to see that with the conditions on the parameters given in (2), both the maps F and T can only have stable cycles,[1] because all the slopes are positive and less than one, so that any possible cycle has an eigenvalue which is necessarily positive and smaller than one. Thus no unstable orbit and also no chaotic behavior can occur.

An important difference between the two maps T and F with positive slopes is that in F *we can*

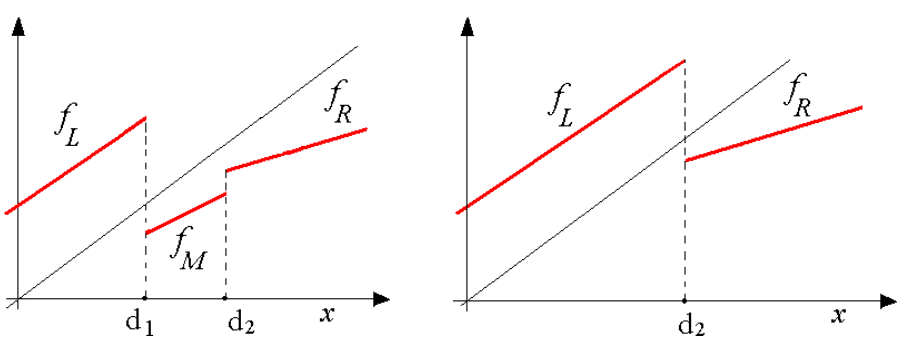

Fig. 1. Qualitative shape of the map under study. (a) Map T with two discontinuity points. (b) Map F.

[1]Except for particular structurally unstable parameter values at which quasiperiodic trajectories, or a Cantor set, exist.

only have one attracting cycle[2] (and, as we shall recall, of any period), whereas in T *we may have two coexisting attracting cycles* (we shall return to this in Sec. 4.2). We only remark that due to the absence of unstable cycles, when two coexisting cycles exist, the separators between the two basins of attraction belong to the set of the discontinuity points and related preimages.

It is well known that a periodic orbit in piecewise smooth maps as T and F may only undergo *border-collision bifurcations.* The term *border-collision* means a contact between a periodic point of a k-cycle, for any $k \geq 1$, with a discontinuity point, which represents a border of its region of definition in the phase space. The term border-collision bifurcation (BCB henceforth) was introduced in [Nusse & Yorke, 1992, 1995] and it is now widely used in this context (i.e. for piecewise smooth maps), although the study and description of such border collision bifurcations started many years ago. In particular, the bifurcations involving discontinuous piecewise linear maps were studied by Leonov already more than fifty years ago, see [Leonov, 1959, 1962], although his pioneering works were known only to a few researchers, among whom are Mira (see [Mira, 1987] and references therein), Maistrenko (see [Maistrenko *et al.*, 1993, 1995, 1998]), and their collaborators.

The BCBs have been widely studied in the last years, mainly because of their relevant applications in engineering (electrical and mechanical). Several works were motivated by models describing particular circuits or models for secure communications [di Bernardo *et al.*, 1999; Banerjee & Grebogi, 1999; Banerjee *et al.*, 2000a, 2000b; Feely *et al.*, 2000; Fournier *et al.*, 2001; Halse *et al.*, 2003; Zhusubaliyev & Mosekilde, 2003; Zhusubaliyev *et al.*, 2006, 2007].

In particular, the bifurcation structure associated with one-dimensional maps having one discontinuity point and increasing/decreasing functions in the two partitions has been the object of recent studies. See [Avrutin *et al.*, 2006; Avrutin & Schanz, 2006; Avrutin *et al.*, 2006; Gardini & Tramontana, 2010], where the so-called increment structure is described. While considering increasing/increasing functions in two partitions (as our map F) the so-called *period adding* structure occurs. As this term is used in the literature in different ways, it is worth to recall that we are using it to refer to the following bifurcation structure: between two periodicity regions (bounded by BCB curves) associated with the existence of cycles with periods p_1 and p_2, there exists a periodicity region associated with the existence of a cycle with period $p_1 + p_2$, and similarly between the regions with periods p_1 and $p_1 + p_2$, there exist regions with periods $2p_1 + p_2$ and $p_1 + 2p_2$, and so on, ad infinitum. The overall bifurcation structure is self-similar, and the rotation numbers of the orbits involved in this structure form the well-known Farey-tree [Hao, 1989], or the Stern–Broccot tree, depending on the used definition of the rotation numbers. Several results were already proved by Leonov [1959, 1962] (also called boxes in file bifurcations in [Mira, 1987]), and a remarkable result was there presented, showing how a recursive process also works for the formulas giving the equations of the BCB curves, which can be explicitly computed in the piecewise linear case. An improvement of this method is given in [Gardini *et al.*, 2010] and its generalization in [Avrutin *et al.*, 2010].

It is worth to emphasize that in all the cited works the period adding structure was reported and investigated in piecewise linear maps with only one discontinuity point (as map F). By contrast, in the present work we prove that this structure also occurs in maps defined on many partitions, involving in this case cycles whose periodic points may be distributed among several partitions (as map T). Moreover, we shall also see that the Leonov's method can still be used.

The study of a discontinuous map with three linear pieces was also involved in the model presented in [Bischi & Merlone, 2009] (related to the works of [Schelling, 1973, 1978], rediscovered after his Nobel Price in economics). That model (considered in [Bischi *et al.*, 2009, 2010]) also dealt with the BCBs involving periodic orbits *belonging to three linear pieces*. However, it has particular restrictions in the parameters, leading to a very specific behavior. By contrast, as we shall see, the bifurcations occurring in the present model, i.e. in the generic map T, are much more complicated. To our knowledge, this is the first time that such an analysis is performed in a piecewise-linear model with two discontinuities, and we shall give the analytic expressions of some BCB curves of the map in (1), under the restrictions on the

[2]As it is proved in [Gardini *et al.*, 2010] (see also [Leonov, 1959]), the existence regions of the stable cycles cannot overlap.

parameters as given in (2). This is, however, just a first step, as the complete bifurcation structure in the eight-dimensional parameter space (also under our restrictions) requires further studies.

The plan of the work is as follows. First, in the next section we recall some relevant results of the map F. Our presentation here is slightly different from that in [Gardini *et al.*, 2010] because we introduce a new notation to characterize the BCB curves, representing the colliding points. This notation refers not only to the periodic orbit undergoing the BCB but also to the specific point of this orbit which collides with the discontinuity point. This new notation is more suitable for a generalization to maps with any number of partitions and a generic discontinuity point, leading directly (as we shall see) to the *concatenation* of the symbolic sequences associated with the cycles. This will be used in Sec. 3 where we prove a generalization of the adding scheme and of Leonov's approach, which will keep the intrinsic power of the method, but can also be applied to maps having more than one discontinuity.

This approach will be extensively used in Sec. 4, where the BCB curves of the map T with two discontinuities will be determined. In fact, after the analysis of the map F in the case of positive slopes (and in the stable regime), a new discontinuity point $d_1 < d_2$ is added and we shall apply the adding scheme to the map T when the cycles have periodic points in three pieces, and BCBs may occur with both discontinuity points. We can immediately appreciate the dynamic difference between the maps (F with one and T with two discontinuity points), from the two-dimensional bifurcation diagram shown in Fig. 2. The bifurcation curves in Fig. 2(a) refer to the (d_1, μ_R) and (d_2, μ_R) parameter planes, and all the other parameters are fixed at the values given above, in (3). For $d_2 > 1.8$ the bifurcation curves are those of the map F (i.e. the regions and BCB curves refer to the (d_2, μ_R) parameter plane), while for $d_1 < \overline{d}_2 = 1.8$ (kept fixed) the bifurcation curves are those of the map T (i.e. the regions and BCB curves refer to the (d_1, μ_R) parameter plane). In Fig. 2(b) we illustrate an enlargement of the upper part of Fig. 1(a).

We shall show how to analytically detect the bifurcation curves related with the dynamics of the map T, using the adding scheme in particular ways, combining the existence of the two discontinuities. The main point is the existence of intersecting BCB

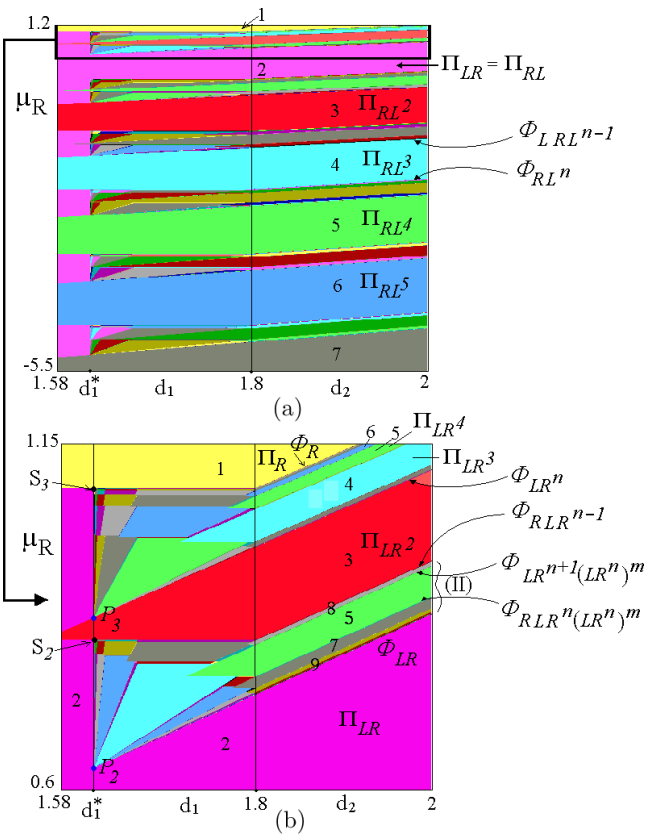

Fig. 2. Bifurcation curves of the map T in the parameter plane (d_1, μ_R) and (d_2, μ_R) as described in the text.

curves associated with the same discontinuity point leading, as in the case of maps with only one discontinuity, to particular points which are called *big-bang bifurcation points*, due to the existence of *infinitely many BCB curves issuing from them*. See, for example, the points P_2 and P_3 in Fig. 2(b) (and infinitely many such points exist). Moreover, the intersection of two BCB curves in which the colliding cycles are associated with two different discontinuity points, leads to a new kind of bifurcation points, which are not issuing points of BCB curves, but *limit sets of a doubly infinite sequence of BCB curves*. See, for example, the points S_2 and S_3 in Fig. 2(b) (and infinitely many such points exist).

In Sec. 4, we describe the BCB curves in several subsections: first those close to the border $\overline{d}_2 = 1.8$ then the periodicity tongues having triangular shape (three boundaries of BCB curves) and finally those having quadrilateral shape (four boundaries of BCB curves).

A final remark in this Introduction refers to the fact that we have not defined the maps F and T in a point of discontinuity. This was done intentionally,

because (as also remarked in [Gardini *et al.*, 2010] and [Avrutin *et al.*, 2010]) this value is not relevant in the analysis of the BCB curves, as the main role is given by the two limiting values of the linear maps involved in the discontinuity points, which play the role of critical points. A different but equivalent way to the purpose of analyzing the bifurcation curves, would be to use a bi-valued function in each discontinuity point, by using the values of the two functions defined on each side of a discontinuity point as values at the discontinuity point.

2. Bifurcation Curves of the Map F

In this section, we give the analytical expressions of the bifurcation curves of the map F, which we rewrite for convenience:

$$x' = F(x) = \begin{cases} f_L(x) = a_L x + \mu_L & \text{if } x < d_2 \\ f_R(x) = a_R x + \mu_R & \text{if } x > d_2 \end{cases} \tag{5}$$

as a function of all the parameters, under the restrictions $0 < a_L < 1$, $0 < a_R < 1$ and $a_L d_2 + \mu_L < a_R d_2 + \mu_R$ [as qualitatively shown in Fig. 1(b)]. The discontinuity point is $x = d_2$ (and in Fig. 2, is shown a two-dimensional bifurcation diagram for $d_2 > 1.8$).In order to find all the families of possible stable cycles, in a simple way, we shall use the Leonov approach, improved as described in [Gardini *et al.*, 2010].

Let us first consider the fixed points of the two branches. The fixed point P_L^* of the left branch f_L is given by $P_L^* = \frac{\mu_L}{1-a_L}$ and exists when it is located in the proper domain, that means for $d_2 > \frac{\mu_L}{1-a_L}$. Otherwise it does not exist, also called a virtual fixed point. When it exists then it clearly attracts at least all points on the left side of d_2. The fixed point P_R^* of the right branch f_R is given by $P_R^* = \frac{\mu_R}{1-a_R}$ and exists when $d_2 < \frac{\mu_R}{1-a_R}$, otherwise it is virtual. When it exists, then it attracts at least all the points on the right side of d_2. Thus in the range

$$\frac{\mu_R}{1-a_R} < d_2 < \frac{\mu_L}{1-a_L} \tag{6}$$

which we are interested in, no fixed point exists. This means that the jump at the discontinuity point d_2 determines the absorbing interval $I = [X_m, X_M]$ inside which the asymptotic dynamics are confined:

$$\begin{gathered} I = [X_m, X_M], \\ X_m = a_R d_2 + \mu_R, \quad X_M = a_L d_2 + \mu_L \end{gathered} \tag{7}$$

where the upper boundary X_M of the absorbing interval is given by the value of the left function at the point of discontinuity $f_L(d_2) = a_L d_2 + \mu_L > d_2$, and the lower boundary X_m by the value of the right function at the same point: $f_R(d_2) = a_R d_2 + \mu_R < d_2$.

As already remarked in the Introduction, notice that the value which is assumed at the discontinuity point $x = d_2$ is of no importance in the description of the possible dynamics, as in any case, points close to d_2 on the left (resp. right) side behave as the point X_M (resp. X_m). Thus the two values $f_L(d_2)$ and $f_R(d_2)$ play the role of critical points independently of which value is assumed for $F(d_2)$.

It is easy to see that any point outside I will be mapped inside I in a finite number of iterations. Therefore the attractor existing inside I represents a global attractor of the map F. This attractor is generally given by a cycle (in limiting cases corresponding to a set in the parameter space with a zero Lebesgue measure, there exist dense periodic points, or quasiperiodic trajectories dense in the absorbing interval, or an invariant Cantor set). The period of the cycle may be any integer number. Moreover, also many cycles with the same period may exist, but with a different number of periodic points on the two sides of the discontinuity point d_2.

2.1. *First level of complexity*

Our next step is to describe which cycles exist, depending on the values of the parameters. We explicitly describe the steps keeping all five parameters (i.e. including the discontinuity point d_2). To find the possible stable cycles we look for *fixed points of the iterated map.* As one can see, the iterated function is again piecewise linear and consists of pieces defined by appropriate compositions of the functions f_L and f_R. Then the simplest cycles to analyze are those called Leonov of first level of complexity (also known in the literature as *principal cycles* or *maximal cycles*). These cycles are characterized by one point in one partition, say on the left side of the discontinuity point (L) and all the other points in the other region, on the right side of d_2 (R). For such a cycle of period $(n+1)$ let us denote the related periodic points as $x_0^* < d_2$, and $x_1^* > \cdots > x_n^* > d_2$. Then x_0^* is a fixed point of the map $f_R^n \circ f_L(x)$and the cycle exists as long as

$$X_m \le x_0^* \le d_2 \tag{8}$$

The equalities denote the BCB leading to the existence of the periodic orbit.

From the iterated map:

$$f_R^n \circ f_L(x) = a_R^n(a_L x + \mu_L) + \mu_R \frac{(1-a_R^n)}{(1-a_R)} \quad (9)$$

and by using the equation $x = f_R^n \circ f_L(x)$ we obtain the periodic point:

$$X_m \le x_0^*$$

$$= \frac{1}{1-a_L a_R^n}\left[a_R^n \mu_L + \mu_R \frac{(1-a_R^n)}{(1-a_R)}\right] \le d_2. \quad (10)$$

The two BCB curves bounding the region of existence of the cycle, say periodicity region Π_{LR^n}, can be both deduced from the two equations associated with (10). Moreover, the inequalities denote on which side of the bifurcation curve the region Π_{LR^n} exists. So that, from $x_0^* \le d_2$ we get:

$$\Pi_{LR^n} : \mu_R \le \frac{[d_2(1-a_L a_R^n) - a_R^n \mu_L](1-a_R)}{(1-a_R^n)} \quad (11)$$

and from $X_m \le x_0^*$, that is $(a_R d_2 + \mu_R) \le x_0^*$, we get:

$$\Pi_{LR^n} : \mu_R \ge \frac{[d_2(1-a_L a_R^n) - a_R^{n-1} \mu_L](1-a_R)}{(1-a_R^{n-1}) + a_L a_R^{n-1}(1-a_R)}. \quad (12)$$

Clearly the related equalities give the BCB curves in the parameter space, and we notice that the periodic point of the cycle is colliding with the discontinuity point d_2 from the left side in the first curve and from the right side in the second one. In this work, however, we are not only interested in the BCB curves, but also explicitly in the characteristics of the colliding points, from which we can detect the BCB curves. To this end, notice that in the first bifurcation curve (obtained from the equality in (11)) the colliding point is exactly x_0^*, associated with the symbolic sequence LR^n, which means that the BCB curve can be detected by using the composite function with that symbolic sequence, and the periodic point is the solution of the equation $f_R^n \circ f_L(x) = x$. For the second BCB curve [obtained from the equality in (12)] the point colliding with d_2 is x_n^*, associated with the first letter in the symbolic sequence RLR^{n-1}. Therefore, the corresponding BCB curve can also be calculated by using the composite function built up according to the sequence RLR^{n-1} and the equation $f_R^{n-1} \circ f_L \circ f_R(d_2) = d_2$. So let us give a name to the BCB curves reflecting the colliding point, as this will be used later:

$$\Phi_{LR^n} : \mu_R = \frac{[d_2(1-a_L a_R^n) - a_R^n \mu_L](1-a_R)}{(1-a_R^n)} \quad (13)$$

$$\Phi_{RLR^{n-1}} : \mu_R = \frac{[d_2(1-a_L a_R^n) - a_R^{n-1} \mu_L](1-a_R)}{(1-a_R^{n-1}) + a_L a_R^{n-1}(1-a_R)}. \quad (14)$$

As one can see, in this notation the side of the collision is directly reflected by the first letter in the symbolic sequence. These BCB curves are straight lines in the parameter plane (d_2, μ_R). For the parameters fixed as in (3) the straight lines of Eqs. (13) and (14) are the boundaries of the principal regions of periods $2, 3, 4 \ldots$ for $d_2 > 1.8$, in Fig. 2(a), above the region of the 2-cycle [better visible in the enlargement of Fig. 2(b)], which accumulate on the line of equation

$$\Phi_R : \mu_R = d_2(1-a_R) \quad (15)$$

above which there is the existence region of the fixed point P_R^*.

There also exist "symmetric cycles", associated with the symbolic sequence RL^n. For these cycles we can order the periodic points as $x_0^* > d_2$, $x_1^* < \cdots < x_n^* < d_2$, reasoning as above. Thus, to determine the BCB curves associated with these cycles, it is enough to replace R and L with L and R, respectively, in the equations given in (13) and (14), obtaining:

$$\Phi_{RL^n} : \mu_L = \frac{[d_2(1-a_R a_L^n) - a_L^n \mu_R](1-a_L)}{(1-a_L^n)} \quad (16)$$

$$\Phi_{LRL^{n-1}} : \mu_L = \frac{[d_2(1-a_R a_L^n) - a_L^{n-1} \mu_R](1-a_L)}{(1-a_L^{n-1}) + a_R a_L^{n-1}(1-a_L)} \quad (17)$$

and, after rearranging, we have:

$$\Phi_{RL^n} : \mu_R = \frac{1}{a_L^n}\left[d_2(1-a_R a_L^n) - \mu_L \frac{(1-a_L^n)}{(1-a_L)}\right] \quad (18)$$

$$\Phi_{LRL^{n-1}} : \mu_R = a_L^n\Bigg[(a_L d_2 + \mu_L)(1-a_R a_L^n) - \mu_L \frac{(1-a_L^n)}{(1-a_L)}\Bigg]. \quad (19)$$

Now the periodic point x_0^* collides with d_2 from the right side, so that the associated symbolic sequence is RL^n, giving the BCB curve Φ_{RL^n}, while the periodic point colliding with the discontinuity from the left side is x_n^*, having the symbolic sequence LRL^{n-1}, and the curve is denoted by $\Phi_{LRL^{n-1}}$. These curves, straight lines in the parameter plane (d_2, μ_R), give the boundaries of the principal regions of periods $2, 3, 4\ldots$ for $d_2 > 1.8$, below the region of the 2-cycle, shown in Fig. 2(a) (the other parameters are fixed as in (3)). The boundaries of the region of the 2-cycle shown in Fig. 2 for $d_2 > 1.8$ are obtained for $n = 1$ from both families of the first level of complexity.

2.2. *Second level of complexity*

It is already known that for any integer $n \geq 1$, between the periodicity regions of the cycles of first level of complexity Π_{LR^n} and $\Pi_{LR^{n+1}}$ of the map F, there exist two infinite sequences of periodicity regions of cycles of the second level of complexity, $\Pi_{(LR^n)^m LR^{n+1}}$ and $\Pi_{LR^n(LR^{n+1})^m}$, for any $m \geq 1$, which accumulated on the boundaries of the periodicity regions of first level between which they are located. The BCB curves can be computed following the approach discussed in [Gardini *et al.*, 2010] by applying the change of variable $y = x - d_2$. However, let us show the application of Leonov's method also in a map with a generic discontinuity point, computing the BCB curves of second complexity level.

Between the curves Φ_{LR^n} and Φ_{RLR^n} we can consider the composite functions associated with the symbolic sequence of the related colliding points LR^n and RLR^n, say

$$T_L = f_R^n \circ f_L, \quad T_R = f_R^n \circ f_L \circ f_R \tag{20}$$

which are applied to points on the left and the right of the discontinuity point d_2, respectively. These maps are still linear, say $T_L = A_L x + B_L$ and $T_R = A_R x + B_R$, where

$$\begin{aligned} A_L &= a_L a_R^n, \\ B_L &= a_R^n \mu_L + \mu_R \frac{(1 - a_R^n)}{(1 - a_R)} \\ A_R &= a_L a_R^{n+1}, \\ B_R &= a_R^n a_L \mu_R + B_L. \end{aligned} \tag{21}$$

Then we can use the equations of the first level of complexity for the map defined by T_L for $x < d_2$ and T_R for $x > d_2$. One family of periodicity regions (having Φ_{LR^n} as limit set) is bounded by the BCB curves given (from (13) and (14)) by:

$$\Phi_{T_L T_R^m} : B_R = \frac{[d_2(1 - A_L A_R^m) - A_R^m B_L](1 - A_R)}{(1 - A_R{}^m)} \tag{22}$$

$$\Phi_{T_R T_L T_R^{m-1}} : B_R = \frac{[d_2(1 - A_L A_R^m) - A_R^{m-1} B_L](1 - A_R)}{(1 - A_R^{m-1}) + A_L A_R^{m-1}(1 - A_R)}. \tag{23}$$

Noting that $\Phi_{T_L T_R^m} = \Phi_{LR^n(RLR^n)^m}, \Phi_{T_R T_L T_R^{m-1}} = \Phi_{RLR^n LR^n(RLR^n)^{m-1}} = \Phi_{RLR^{n-1}(RLR^n)^m}$, and substituting the explicit expressions of the coefficients in (21) we have the BCB curves of second complexity level in explicit form:

$$\begin{aligned} &\Phi_{LR^n(RLR^n)^m} : a_R^n(\mu_L + a_L \mu_R) + \mu_R \frac{(1 - a_R^n)}{(1 - a_R)} \\ &= \frac{\left[d_2(1 - a_L a_R^n (a_L a_R^{n+1})^m) - (a_L a_R^{n+1})^m \left(a_R^n \mu_L + \mu_R \frac{(1 - a_R^n)}{(1 - a_R)} \right) \right] (1 - a_L a_R^{n+1})}{1 - (a_L a_R^{n+1})^m} \end{aligned} \tag{24}$$

and

$$\begin{aligned} &\Phi_{RLR^{n-1}(RLR^n)^m} : a_R^n a_L \mu_R + a_R^n \mu_L + \mu_R \frac{(1 - a_R^n)}{(1 - a_R)} \\ &= \frac{\left[d_2(1 - a_L a_R^n (a_L a_R^{n+1})^m) - (a_L a_R^{n+1})^{m-1} \left(a_R^n \mu_L + \mu_R \frac{(1 - a_R^n)}{(1 - a_R)} \right) \right] (1 - a_L a_R^{n+1})}{(1 - (a_L a_R^{n+1})^{m-1}) + a_L a_R^n (a_L a_R^{n+1})^{m-1}(1 - a_L a_R^{n+1})} \end{aligned} \tag{25}$$

which can also be written as

$$\Phi_{LR^n(RLR^n)^m} : \mu_R = d_2(1-a_R) + \frac{d_2(1-a_L)-\mu_L}{\dfrac{a_L H'}{1+H'} + \dfrac{1-a_R^n}{(1-a_R)a_R^n}} \tag{26}$$

and

$$\Phi_{RLR^{n-1}(RLR^n)^m} : \mu_R = d_2(1-a_R) + \frac{d_2(1-a_L)-\mu_L}{\dfrac{a_L H''}{1+H''} + \dfrac{1-a_R^n}{(1-a_R)a_R^n}} \tag{27}$$

where

$$H' = \frac{1-A_L^m}{(1-A_R)A_R^m}, \quad H'' = A_R + \frac{1-A_R^{m-1}}{(1-A_R)A_R^{m-1}}. \tag{28}$$

Similarly from (16) and (17) we obtain, after substitution and rearranging:

$$\Phi_{LR^{n+1}(LR^n)^m} : \mu_R = d_2(1-a_R) + \frac{d_2(1-a_L)-\mu_L}{\dfrac{a_L}{1+S''} + \dfrac{1-a_R^n}{(1-a_R)a_R^n}} \tag{29}$$

$$\Phi_{RLR^n(LR^n)^m} : \mu_R = d_2(1-a_R) + \frac{d_2(1-a_L)-\mu_L}{\dfrac{a_L}{1+S'} + \dfrac{1-a_R^n}{(1-a_R)a_R^n}} \tag{30}$$

where

$$\begin{aligned} S' &= \frac{1-A_L^m}{(1-A_L)A_L^m}, \\ S'' &= A_R + \frac{1-A_L^{m-1}}{(1-A_L)A_L^{m-1}} \end{aligned} \tag{31}$$

giving the explicit equations of the second family of BCB curves of second level, having Φ_{RLR^n} as limit set. Clearly, companion families of second level, between the BCB curves Φ_{RL^n} and Φ_{LRL^n}, also exist, and the related BCB curves can be obtained from the equations above, exchanging L and R and vice versa. A few bifurcation curves of second complexity level of map F in the plane (d_2, μ_R) are drawn in Fig. 2(b) (a few more in Fig. 7(b) of Sec. 4.1).

In this work we are mainly interested in the bifurcations occurring in the map with two discontinuity points, and in the following we shall refer to the enlargement of Fig. 2(b). However, it is clear that similar reasoning can be repeated in the regions below, by self-similar behavior. In fact, as it is immediate to see from Fig. 2(a), the bifurcation structure between the periodicity regions of the 2-cycle and that of the fixed point in the R side are repeated (with an obvious change in the periods) between any pair of regions $\Pi_{RL^{n+1}}$ and Π_{RL^n}, below the one here considered.

Let us first describe, in the next section, how the adding scheme can be used in a generalized context (as we shall do in Sec. 4 with two discontinuities).

3. Adding Scheme for a Map on Many Partitions

In the case of a map with one discontinuity point, a commonly used way to describe the period adding structure is based on the symbolic dynamics. In this case, the procedure is as follows: denote sequences corresponding to cycles with periods p_1 and p_2 as σ and ρ, and the corresponding existence regions as $\Pi(\sigma)$ and $\Pi(\rho)$. Then, between $\Pi(\sigma)$ and $\Pi(\rho)$ there exists the region $\Pi(\sigma\rho)$, between $\Pi(\sigma)$ and $\Pi(\sigma\rho)$ there exists the region $\Pi(\sigma^2\rho)$, and so on. It is easy to see that both the addition of the periods of the involved cycles and the Farey-addition[3] of the corresponding rotation numbers are direct consequences of the concatenation of the symbolic sequences. The infinite directed graph consisting of all sequences corresponding to the cycles in a period

[3]Defined by the rule $\frac{a}{b} \oplus \frac{c}{d} = \frac{a+c}{b+d}$.

adding structure is also called the (*Farey-tree like*) *symbolic sequence adding scheme*, and the sequences σ and ρ defining the starting nodes of this graph as its *starting sequences*.

As remarked in the introduction, an important result regarding the symbolic sequence adding scheme was contributed already by Leonov [1959]. He introduced an interior structuring of the symbolic sequence adding scheme based on the following *recursive* process. Let σ and ρ be the starting sequences (in fact, Leonov considered only the case $\sigma = L$ and $\rho = R$, but this does not represent any restriction of the generality). Then the sequences from the two infinite families $\{\sigma^n\rho \,|\, n > 0\}$ and $\{\sigma\rho^n \,|\, n > 0\}$ are called the sequences of the *first level of complexity*. The key point of the recursive structuring is to note that for any $k \geq 0$ between two subsequent sequences ϖ_n and ϖ_{n+1} of the kth level of complexity there exist two infinite families $\{(\varpi_n)^m\varpi_{n+1} \,|\, m > 0\}$ and $\{\varpi_{n+1}(\varpi_n)^m \,|\, m > 0\}$ [the sequences of these families are called sequences of the $(k+1)$th *level of complexity*]. The advantage of this recursive structuring of the symbolic sequence adding scheme is due to the fact that it can be used not only for determining the sequences involved into the symbolic sequence adding scheme but *also for the calculation of the corresponding bifurcation curves*. For the particular case of piecewise linear maps the resulting expressions can be written in explicit form. This calculation procedure is reported with some simplification compared with the original Leonov's approach (avoiding an unnecessary coordinate transformation) in [Gardini *et al.*, 2010] and then, in a generalized form (not related to the period adding bifurcation structures) in [Avrutin *et al.*, 2010]. It is demonstrated in these works that it is much more efficient than the usual calculation procedures and allows to explicitly obtain much more bifurcation curves.

Up to now, this technique has only been applied to maps with one discontinuity point (as map F), so that the existing cycles have periodic points which belong to the two partitions of the map. In our case, the map T has three linear pieces, and we shall describe the bifurcation structure associated with cycles having periodic points in all three partitions.

The main point in the use of the adding scheme is to recognize when it can be applied. That is, given any two cycles (with periods p_1 and p_2 and related sequences σ and ρ), when can we say that these can be used as *starting sequences* to get the complete adding scheme? Our theorem answers this question. We give sufficient conditions to apply the adding scheme to discontinuous maps, independently of the number of discontinuity points. Then the complete binary tree can be computed, associated with the existence of related periodic orbits. Also the Leonov's method for the computation of the BCB curves still works. However, it is worth to note that in the case of two or more discontinuity points, the cycles so determined in the complete tree have no longer a direct relation with the rotation numbers.[4]

3.1. *Main theorem*

As already mentioned, until now the applicability of the symbolic sequence adding scheme for the description of the period adding structures was known for maps defined on two partitions. Below, we demonstrate that the number of partitions on which the map is defined is not significant. In fact, the sufficient condition for the occurrence of the period adding structure following the symbolic sequence adding scheme is related with *the existence of two stable cycles undergoing border collision bifurcations at the same parameter values and colliding with the same discontinuity*. Thus, it is not necessary to have a map f with only one discontinuity. The main point is that two BCB curves of stable cycles, characterized by collisions on opposite sides of the same discontinuity point, are intersecting [as qualitatively shown in Fig. 3(c)]. Then infinitely many BCB curves issue from the intersection point P, which is a so-called *big bang bifurcation point*. Let us prove the following.

Theorem 1. *Let $x' = f(x)$ be a piecewise linear map whose components have slopes all belonging to the interval $(0, 1)$, and assume the existence of two BCB curves $\Phi_{\overline{L}}$ and $\Phi_{\overline{R}}$ in a parameter plane,*

[4]When dealing with maps defined on many partitions the concept of rotation number needs to be basically reconsidered. For example, for a k-periodic orbit of the map T considered in this work associated with three partitions labeled L, M and R we can define the number of periodic points in the three partitions, say n_L, n_M, n_R, with $k = n_L + n_M + n_R$, and also the fractions n_i/k (for $i = L, M, R$). However, it must still be investigated whether this is useful and how. This argument is not considered in this work.

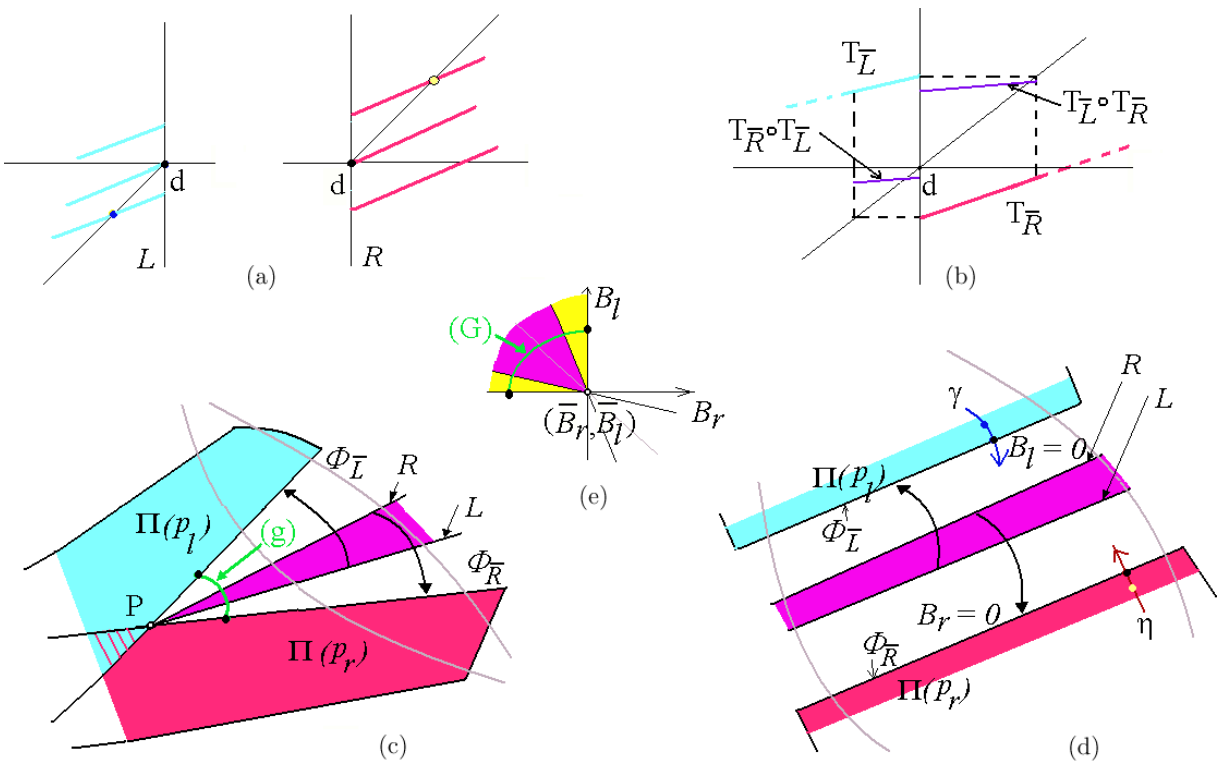

Fig. 3. Qualitative description of the map $\overline{T}$ in (33), and qualitative representation of the parameter plane, under the assumptions of the theorem, as explained in the text.

boundaries of two overlapping periodicity regions, intersecting at a point P, and related to the collision with a discontinuity in $x = d$ of two different cycles of f from the left and right, respectively. Then infinitely many BCB curves originate from the point P. The symbolic sequences corresponding to the orbits undergoing these BCBs can be determined using the adding scheme with the starting sequences $\overline{L}$ and $\overline{R}$.

Let us consider two different periodicity regions, $\Pi(p_l)$ and $\Pi(p_r)$, as qualitatively shown in Fig. 3(c), having an overlapping region. For parameters belonging to the boundary $\Phi_{\overline{L}}$ the cycle has a periodic point x_l^* (of period p_l) colliding with the discontinuity point $x = d$ from the left, while at the other BCB curve $\Phi_{\overline{R}}$ the periodic point x_r^* (of period p_r) collides with d from the right. Let us define as $T_{\overline{L}}$ (resp. $T_{\overline{R}}$) the composite function which gives the periodic point colliding with d from the left (resp. right):

$$\begin{aligned} T_{\overline{L}}(x) &= f_{\sigma_{p_l}} \circ \cdots \circ f_{\sigma_1}(x) \\ T_{\overline{R}}(x) &= f_{\rho_{p_r}} \circ \cdots \circ f_{\rho_1}(x) \end{aligned} \tag{32}$$

where σ_i (with $i = 1, \ldots, p_l$) and ρ_j (with $j = 1, \ldots, p_r$) are the suitable letters, giving the symbolic sequence of the colliding point of the cycles with periods p_l and p_r for map f. It is worth to emphasize that we are not making any assumptions regarding the specific letters in the symbolic sequence σ and ρ except for the first letters in these sequences. By our assumptions, the first letter in $\overline{L} = \sigma_1 \cdots \sigma_{p_l}$, that is σ_1, must correspond for f to the partition located directly *on the left side* of the discontinuity point d. Similarly, the first letter in $\overline{R} = \rho_1 \cdots \rho_{p_r}$ corresponds to the partition located directly *on the right side* of the discontinuity point d. All other letters σ_i (with $i = 2, \ldots, p_l$) and ρ_j (with $j = 2, \ldots, p_r$) may be arbitrary and correspond to any partition of f. By our definition the composite functions $T_{\overline{L}}$ and $T_{\overline{R}}$ collapse periodic points of f to fixed points, that means $T_{\overline{L}}(x_r^*) = x_r^*$ and $T_{\overline{R}}(x_l^*) = x_l^*$. As a consequence, when the parameters belong to the BCB curve $\Phi_{\overline{L}}$ (resp. $\Phi_{\overline{R}}$) we have $T_L(d) = d$ (resp. $T_{\overline{R}}(d) = d$).

Then, we consider the map $\overline{T}$ defined via the two functions $T_{\overline{L}}$ and $T_{\overline{R}}$ as follows:

$$x' = \overline{T}(x),$$

$$\overline{T}(x) = \begin{cases} T_{\overline{L}}(x) = f_{\sigma_{p_l}} \circ \cdots \circ f_L(x) \\ \qquad = A_l x + B_l & \text{if } x < d \\ T_{\overline{R}}(x) = f_{\rho_{p_r}} \circ \cdots \circ f_R(x) \\ \qquad = A_r x + B_r & \text{if } x > d \end{cases} \tag{33}$$

where $A_l \in (0,1)$ and $A_r \in (0,1)$. Considering the qualitative shape of a composite map, for example, $T_{\overline{L}}(x)$, when the parameters cross the related periodicity regions we can state that the shape of the map defined by $T_{\overline{L}}$ (resp. $T_{\overline{R}}$) for $x < d$ (resp. $x > d$) is locally (in a neighborhood of the discontinuity point $x = d$) as reported in Fig. 3(a), where we have used blue (resp. red) colors for the branches. The figure shows the shapes of the functions in the three possible situations when the fixed points exist, collide, and do not exist. Crossing the BCB curves through an arc γ (resp. η) as shown in Fig. 3(d), the shapes of the composite functions change as shown in Fig. 3(a).

When a parameter point belongs to the overlapping region $\Pi(p_l) \cap \Pi(p_r)$ both cycles exist, while inside the nonoverlapping parts of the regions $\Pi(p_l)$ and $\Pi(p_r)$ only one of these cycles exists, and they both do not exist when a parameter point belongs to the region between the two curves $\Phi_{\overline{L}}$ and $\Phi_{\overline{R}}$.

At the point P where the two BCB curves $\Phi_{\overline{L}}$ and $\Phi_{\overline{R}}$ are intersecting we have both $(B_l + A_l d) = d$ and $(B_r + A_r d) = d$, thus the map $\overline{T}$ is continuous at the point $x = d$. In the two-dimensional parameter plane (B_r, B_l) the point P corresponds to $(B_r, B_l) = (\overline{B_r}, \overline{B_l})$ where $\overline{B_r} = d(1 - A_r)$ and $\overline{B_l} = d(1 - A_l)$.

From the continuity of $\overline{T}$ in $x = d$ when the parameters are in P, we have that considering a point between the periodicity regions, in a neighborhood of P, the qualitative shape of the map is as shown in Fig. 3(b). That is, we necessarily have $(B_l + A_l d) > d$ and $(B_r + A_r d) < d$. Therefore, we can define an absorbing interval $I = [T_{\overline{R}}(d), T_{\overline{L}}(d)] = [B_r + A_r d, B_l + A_l d]$, inside which the map (with two increasing branches) is confined. According to our assumptions no unstable cycle can exist, thus the attracting set in I can be a periodic orbit or there exist quasiperiodic orbits or an Invariant Cantor set.

The proof of Theorem 1 is performed in three steps. First, we prove the existence of a region associated with a two cycle of $\overline{T}$, then, in Step 2 we prove that the arguments can be repeated, showing the existence of two infinite families of periodicity regions associated with cycles having the symbol sequence $\overline{L}\overline{R}^m$, for any $m > 1$, having $\Phi_{\overline{R}}$ as limit set, and $\overline{R}\overline{L}^m$, $m > 1$, having $\Phi_{\overline{L}}$ as limit set. These two families are of first level of complexity. Then in Step 3 we state that all the complexity levels exist.

Step 1. Let us first show that moving the parameter point along an arc (g) as qualitatively shown in Fig. 3(c), close enough to P, we must necessarily cross the periodicity region of a 2-cycle of $\overline{T}$. To prove this, let us consider the second iterate of $\overline{T}$, i.e. the map $\overline{T}^2$ given by

$$\begin{cases} T_{\overline{R}} \circ T_{\overline{L}}(x) = A_r A_l x + (B_r + A_r B_l) & \text{if } x < d \\ T_{\overline{L}} \circ T_{\overline{R}}(x) = A_r A_l x + (B_l + A_l B_r) & \text{if } x > d \end{cases} \tag{34}$$

then the graph of $\overline{T}^2$ on the left side of d is a line (with positive slope and smaller than those of $\overline{T}$) connecting the points $((B_r + A_r d), T_{\overline{R}} \circ T_{\overline{L}}(B_r + A_r d))$ and $(d, T_{\overline{R}} \circ T_{\overline{L}}(d))$, where

$$\begin{aligned} T_{\overline{R}} \circ T_{\overline{L}}(d) &= A_r A_l d + (B_r + A_r B_l) \\ T_{\overline{R}} \circ T_{\overline{L}}(B_r + A_r d) &= A_r A_l (B_r + A_r d) \\ &\quad + (B_r + A_r B_l). \end{aligned} \tag{35}$$

Notice that if the parameter point moves along a path as (g) in Fig. 3(c), from a point belonging to $\Phi_{\overline{L}}$ (where $(B_l + A_l d) = d$ and $(B_r + A_r d) < d$) approaching the other BCB curve, the value of $(B_l + A_l d)$ increases, $(B_l + A_l d) > d$, and once that parameter point reaches the curve $\Phi_{\overline{R}}$ we have $(B_r + A_r d) = d$. Thus the parameter point (B_r, B_l) must cross the quadrant along a path (G) as schematically shown in Fig. 3(e).

Then the sufficient conditions which guarantee that $\overline{T}^2$ has a fixed point on the left side are:

$$\begin{aligned} T_{\overline{R}} \circ T_{\overline{L}}(d) &= (B_r + A_r B_l) \\ &\quad + A_r A_l d < d \end{aligned} \tag{36}$$

$$\begin{aligned} T_{\overline{R}} \circ T_{\overline{L}}(B_r + A_r d) &= (B_r + A_r B_l) \\ &\quad + A_r A_l (B_r + A_r d) \\ &> (B_r + A_r d). \end{aligned} \tag{37}$$

This second condition is fulfilled for $B_l + A_l(B_r + A_r d) > d$, that is, for $(B_l + A_l B_r) + A_r A_l d > d$. Thus both the inequalities in (36) and (37) are satisfied

when

$$-A_l B_r + d(1 - A_r A_l) < B_l < \frac{1}{A_r}[-B_r + d(1 - A_r A_l)] \quad (38)$$

which is a cone crossing the quadrant of interest of the plane (B_r, B_l) (as $A_l < 1$ and $\frac{1}{A_r} > 1$), as qualitatively shown in Fig. 3(e), so that this region must necessarily be crossed from the arc (G).

Clearly we get analogous results for the map $T_{\overline{L}} \circ T_{\overline{R}}(x)$. It is enough to replace $\overline{R}$ and $\overline{L}$ with $\overline{L}$ and $\overline{R}$, respectively, and exchange the inequalities, to see that the conditions are satisfied in the same region, and thus also a fixed point for $T_{\overline{L}} \circ T_{\overline{R}}$ exists on the right side of d.

Summarizing, under the given assumptions, we have seen that between the two boundaries $\Phi_{\overline{L}}$ and $\Phi_{\overline{R}}$ a 2-cycle of $\overline{T}$ exists, with periodic points given by the fixed point equations $T_{\overline{R}} \circ T_{\overline{L}}(x) = x$ and $T_{\overline{L}} \circ T_{\overline{R}}(x) = x$. Notice that the two equations

$$\Phi_{\overline{L}\overline{R}} : B_l = -A_l B_r + d(1 - A_r A_l) \quad (39)$$

$$\Phi_{\overline{R}\overline{L}} : B_l = \frac{1}{A_r}[-B_r + d(1 - A_r A_l)] \quad (40)$$

give the BCB curves of the 2-cycle of $\overline{T}$. In fact, the parameters at which a BCB occurs for the 2-cycle are given by $T_{\overline{R}} \circ T_{\overline{L}}(d) = d$, which corresponds to the first equation, and by $T_{\overline{L}} \circ T_{\overline{R}}(d) = d$, which corresponds to the second one.

Moreover, from the fact that when the parameter point is on $\Phi_{\overline{L}}$ (where $(B_l + A_l d) = d$) we have $T_{\overline{R}} \circ T_{\overline{L}}(B_r + A_r d) < T_{\overline{R}} \circ T_{\overline{L}}(d) < d$, we can state that in the region between $\Phi_{\overline{L}}$ and the periodicity region of the 2-cycle this sign is kept, and thus the BCB at which we have $T_{\overline{R}} \circ T_{\overline{L}}(d) = d$ (BCB where the boundary d collides from the left side) corresponds to the boundary of the periodicity region of the 2-cycle *farthest* from $\Phi_{\overline{L}}$, as shown in Figs. 3(c) and 3(d). The other one is clearly a BCB where the boundary d collides from the right side.

Thus the symbolic sequence of the 2-cycle so obtained is $\overline{L}\overline{R}$ (or $\overline{R}\overline{L}$ as it is cyclic invariant), however it is important to recall that the BCB curve of equation $T_{\overline{R}} \circ T_{\overline{L}}(d) = d$ is associated with the periodic point having symbolic sequence $\overline{L}\overline{R}$ while the other BCB curve of equation $T_{\overline{L}} \circ T_{\overline{R}}(d) = d$ to the symbolic sequence $\overline{R}\overline{L}$. In terms of the starting symbolic sequences associated with the original map f, to get the symbolic sequence of the new cycle we have to concatenate the two starting sequences, substituting the symbolic sequence $\sigma_1 \cdots \sigma_{p_l}$ to $\overline{L}$ and $\rho_1 \cdots \rho_{p_r}$ to $\overline{R}$, so that $\overline{L}\overline{R} = \sigma_1 \cdots \sigma_{p_l} \rho_1 \cdots \rho_{p_r}$ and $\overline{R}\overline{L} = \rho_1 \cdots \rho_{p_r} \sigma_1 \cdots \sigma_{p_l}$.

Step 2. Now, considering the periodicity region of the 2-cycle determined above, say $\Pi(\overline{L}\overline{R})$, along a path crossing $\Pi(\overline{L}\overline{R})$ as shown in Fig. 4: the shape

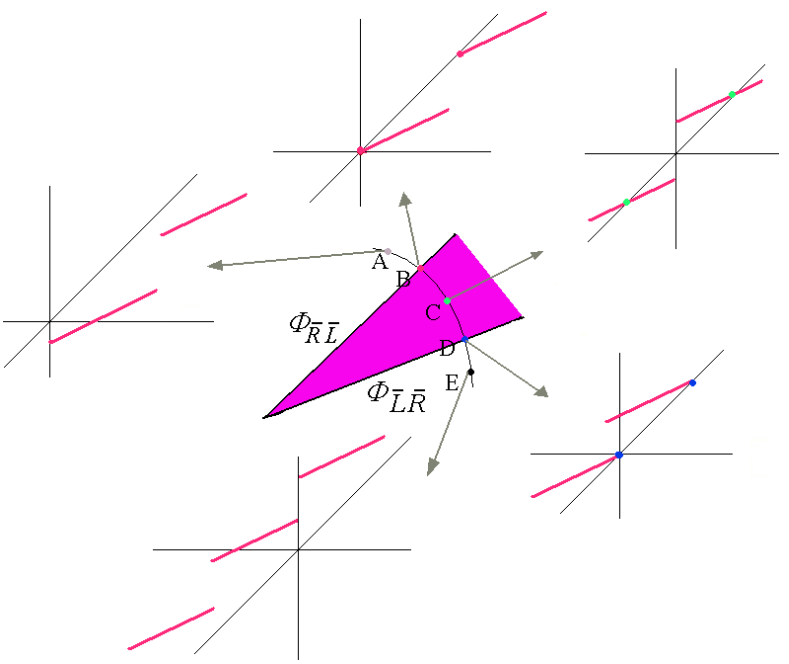

Fig. 4. Qualitative description of the map $\overline{T}^2$ at different points of the parameter plane crossing the periodicity region $\Pi(\overline{L}\overline{R})$.

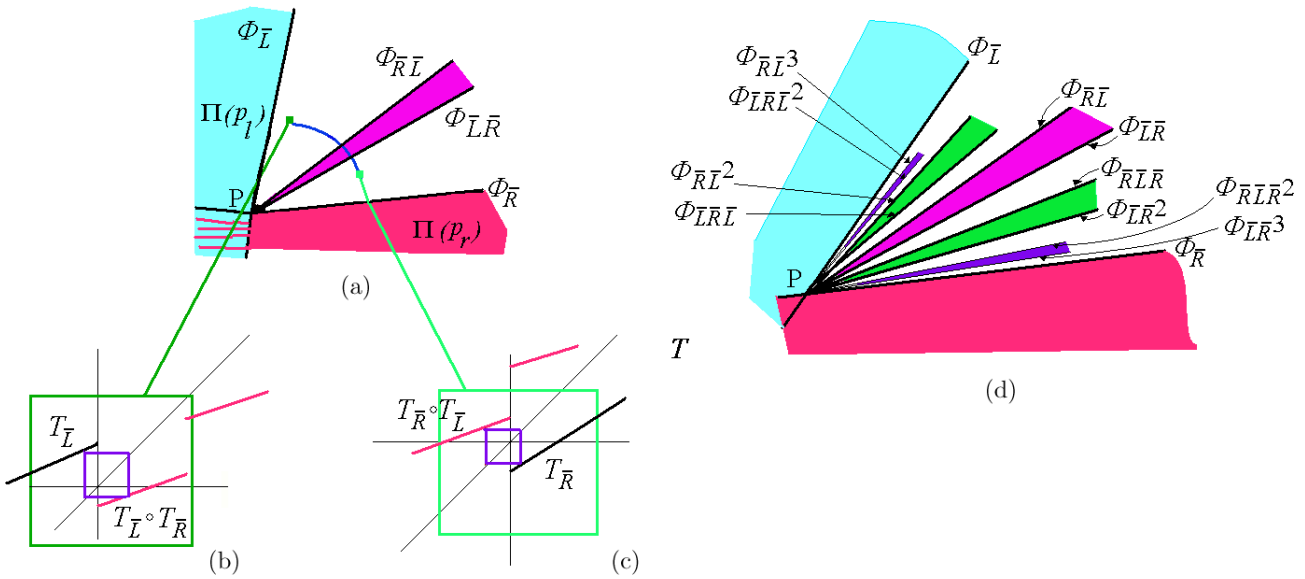

Fig. 5. Qualitative representation in the parameter plane of the periodicity regions, as explained in the text.

of the map $\overline{T}^2$ changes as schematically shown in the same picture. It follows that when considering a point close enough to P between the BCB curves $\Phi_{\overline{L}}$ and $\Phi_{\overline{R}\,\overline{L}}$ as shown in dark green in Fig. 5(a), then the branches of the map defined as

$$\begin{aligned} T_{\overline{L}}(x) &= A_l x + B_l && \text{if } x < d \\ T_{\overline{L}} \circ T_{\overline{R}}(x) &= A_r A_l x + (B_l + A_l B_r) && \text{if } x > d \end{aligned} \tag{41}$$

have the qualitative shape reported in the green rectangle of Fig. 5(b). Here, we can use the same arguments considered above (in Step 1), to prove that a 2-cycle of this map must exist in a proper periodicity region between the two starting BCB curves. The region of existence of this 2-cycle corresponds, for the map in (33), to a cycle of period 3 with symbolic sequence $\overline{R}\overline{L}^2$ (and for the original map f, it is obtained substituting the symbolic sequence $\sigma_1 \cdots \sigma_{p_l}$ to $\overline{L}$ and $\rho_1 \cdots \rho_{p_r}$ to $\overline{R}$). The two BCB curves at the boundaries are given by:

$$\begin{aligned} &\Phi_{\overline{R}\overline{L}^2} : T_{\overline{L}}^2 \circ T_{\overline{R}}(d) = d \\ &\Phi_{\overline{L}\overline{R}\overline{L}} : T_{\overline{L}} \circ T_{\overline{R}} \circ T_{\overline{L}}(d) = d. \end{aligned} \tag{42}$$

Similarly, considering a point close enough to P between the BCB curves $\Phi_{\overline{L}\overline{R}}$ and $\Phi_{\overline{R}}$ as shown in light green in Fig. 5(a), the branches of the map defined as

$$\begin{aligned} T_{\overline{R}} \circ T_{\overline{L}}(x) &= A_r A_l x + (B_r + A_r B_l) && \text{if } x < d \\ T_{\overline{R}}(x) &= A_r x + B_r && \text{if } x > d \end{aligned} \tag{43}$$

have the qualitative shape reported in the green rectangle of Fig. 5(c), and as before we can state that a 2-cycle of this map must exist in a proper periodicity region between the two starting BCB curves. The region of existence of this 2-cycle corresponds, for the map $\overline{T}$ in (33), to a cycle of period 3 with symbolic sequence $\overline{L}\overline{R}^2$ (and for the original map f it is obtained by substituting the symbolic sequence $\sigma_1 \cdots \sigma_{p_l}$ to $\overline{L}$ and $\rho_1 \cdots \rho_{p_r}$ to $\overline{R}$). The two BCB curves at the boundaries are given by:

$$\begin{aligned} &\Phi_{\overline{L}\overline{R}^2} : T_{\overline{R}}^2 \circ T_{\overline{L}}(d) = d \\ &\Phi_{\overline{R}\overline{L}\overline{R}} : T_{\overline{R}} \circ T_{\overline{L}} \circ T_{\overline{R}}(d) = d. \end{aligned} \tag{44}$$

Thus the two green regions shown in Fig. 5(d) have been proved to exist, with the symbolic sequence as given above.

It is clear that we can continue reasoning in a similar way. In each step we construct new maps analogous to (41) and (43) and prove for these maps the existence of a 2-cycle as well as the location of the corresponding region in the parameter space. That is, considering (for any $k \geq 1$) the map defined as

$$T_{\overline{L}}(x) \quad \text{if } x < d, \qquad T_{\overline{L}}^k \circ T_{\overline{R}}(x) \quad \text{if } x > d \tag{45}$$

we can prove the existence of a 2-cycle, leading to a cycle of period $(k+2)$ of $\overline{T}$. Similarly considering (for any $k \geq 1$) the map defined as

$$T_{\overline{R}}^k \circ T_{\overline{L}}(x) \quad \text{if } x < d, \qquad T_{\overline{R}}(x) \quad \text{if } x > d. \tag{46}$$

So we are led to find two families of periodicity regions, associated with cycles of $\overline{T}$ having the symbolic sequence $\overline{R}\overline{L}^m$ (accumulating on the BCB curve $\Phi_{\overline{L}}$) for any $m \geq 1$ and $\overline{L}\overline{R}^m$ (accumulating on the BCB curve $\Phi_{\overline{R}}$) for any $m \geq 1$ (for $m = 1$ the two families give the same periodicity region).

Between the two BCB curves $\Phi_{\overline{L}}$ and $\Phi_{\overline{R}\overline{L}}$ we have the two BCB curves $\Phi_{\overline{L}\overline{R}\overline{L}}$ and $\Phi_{\overline{R}\overline{L}^2}$ in the order shown in Fig. 5(d); between the two BCB curves $\Phi_{\overline{L}\overline{R}}$ and $\Phi_{\overline{R}}$ there exist two BCB curves $\Phi_{\overline{L}\overline{R}^2}$ and $\Phi_{\overline{R}\overline{L}\overline{R}}$; between the two BCB curves $\Phi_{\overline{L}}$ and $\Phi_{\overline{R}\overline{L}^2}$ we have the two BCB curves $\Phi_{\overline{L}\overline{R}\overline{L}^2}$ and $\Phi_{\overline{R}\overline{L}^3}$ in the order shown in Fig. 5(d), and so on iteratively.

Summarizing, we have that for any $m \geq 1$ the cycles of the family $\overline{L}\overline{R}^m$ exist and the two BCB curves of the periodicity region $\Pi_{\overline{L}\overline{R}^m}$ (accumulating on the BCB curve $\Phi_{\overline{R}}$) are given by the following equations:

$$\Phi_{\overline{L}\overline{R}^m} : T_{\overline{R}}^m \circ T_{\overline{L}}(d) = d \tag{47}$$

$$\Phi_{\overline{R}\overline{L}\overline{R}^{m-1}} : T_{\overline{R}}^{m-1} \circ T_{\overline{L}} \circ T_{\overline{R}}(d) = d \tag{48}$$

and similarly for $m > 1$ the cycles of the family $\overline{R}\overline{L}^m$ exist and the two BCB curves of the periodicity region $\Pi_{\overline{R}\overline{L}^m}$ are given by (changing $\overline{L}$ and $\overline{R}$ into $\overline{R}$ and $\overline{L}$, respectively)

$$\Phi_{\overline{R}\overline{L}^m} : T_{\overline{L}}^m \circ T_{\overline{R}}(d) = d \tag{49}$$

$$\Phi_{\overline{L}\overline{R}\overline{L}^{m-1}} : T_{\overline{L}}^{m-1} \circ T_{\overline{R}} \circ T_{\overline{L}}(d) = d. \tag{50}$$

So far we have proved for the map (33), the existence of the periodicity regions of cycles associated with symbolic sequence with the *first level of complexity*.

Step 3. Then we can continue in a similar way: between any pair of subsequent periodicity regions of first level, close enough to P, the shape of the map is the same and we can repeat the two steps described above and summarized in Fig. 5. For example, between the two periodicity regions $\Pi_{\overline{L}\overline{R}^n}$ and $\Pi_{\overline{L}\overline{R}^{n+1}}$, we have to consider the two BCB curves given by $\Phi_{\overline{L}\overline{R}^n}$ (on which the n-cycle has a periodic point colliding from the left side of d) and by $\Phi_{\overline{R}\overline{L}\overline{R}^n}$ (on which the $(n+1)$-cycle has a periodic point colliding from the right side of d). This means that we have to consider the function $T_{\overline{R}}^n \circ T_{\overline{L}}(x)$ for $x < d$, and the function $T_{\overline{R}}^n \circ T_{\overline{L}} \circ T_{\overline{R}}(x)$ for $x > d$, and via Steps 1 and 2 used above, we obtain the existence of the two families of periodicity regions (between $\Phi_{\overline{L}\overline{R}^n}$ and $\Phi_{\overline{R}\overline{L}\overline{R}^n}$) of cycles of *second level of complexity*, with symbolic sequences $\overline{L}\overline{R}^n(\overline{R}\overline{L}\overline{R}^n)^m$ and $\overline{R}\overline{L}\overline{R}^n(\overline{L}\overline{R}^n)^m$.

The process can be continued iteratively, as at each step the new periodicity regions so created are between the two starting ones, leaving an empty space where we can continue. Thus the process can never end, leading to the BCB curves of any complexity level, always bounding periodicity regions associated with a stable cycle of the map $\overline{T}$.

Apart from the periodicity regions, the residual set (limit set of BCB curves) corresponds to parameters associated with irrational rotation numbers and an invariant Cantor set. We have so proved our theorem, leading to the existence of a whole fan of periodicity regions issuing from the crossing point P, bounded by BCB curves of any complexity level, densely filling the region between the curves $\Phi_{\overline{L}}$ and $\Phi_{\overline{R}}$.

The reader can realize that the structure of Fig. 5(d) is that one observed in Fig. 2 issuing from the points P_2 and P_3, and this will be discussed in Sec. 4. Let us first show, in the next subsection, that Leonov's approach can be applied to compute the explicit equations of the BCB curves.

3.2. *BCB curves and Leonov's method*

We recall that under our assumptions, moving the parameters along the path (g) as in Fig. 3(c), the map $\overline{T}$ in (33) has the qualitative shape described in Fig. 3(b), then the existence of the stable cycles was also proved in a theorem by [Keener, 1980]. However, it is worth to note that the theorem proved above not only guarantees the existence of the period adding structure issuing from the intersection point of two border collision bifurcation curves but also provides us with an analytical framework for the calculation of the border collision bifurcation curves bounding the periodicity regions forming this structure. Indeed, since the map we are considering is piecewise linear, the implicit equations of first complexity level in (47) and (48) can be written also in explicit form:

$$\Phi_{\overline{L}\overline{R}^m} : B_r = \frac{[d(1 - A_l A_r^m) - A_r^m B_l](1 - A_r)}{(1 - A_r^m)} \tag{51}$$

$$\Phi_{\overline{R}\overline{L}\overline{R}^{m-1}} : B_r = \frac{[d(1-A_lA_r^m) - A_r^{m-1}B_l](1-A_r)}{(1-A_r^{m-1}) + A_lA_r^{m-1}(1-A_r)}. \tag{52}$$

Clearly Eqs. (49) and (50) can easily be obtained by using the symmetric property, and are given explicitly by:

$$\Phi_{\overline{R}\overline{L}^m} : B_l = \frac{[d(1-A_rA_l^m) - A_l^mB_r](1-A_l)}{(1-A_l^m)} \tag{53}$$

$$\Phi_{\overline{L}\overline{R}\overline{L}^{m-1}} : B_l = \frac{[d(1-A_rA_l^m) - A_l^{m-1}B_r](1-A_l)}{(1-A_l^{m-1}) + A_rA_l^{m-1}(1-A_l)}. \tag{54}$$

Moreover, besides the BCB curves of the periodicity regions of cycles of first level, we can have the explicit equations of the BCB curves of any level of complexity. This can be obtained, for example, following *Leonov's approach* (as proposed in [Gardini *et al.*, 2010]), which consists of a map on the coefficients leading from BCB curves of a level k to those of the next level $k+1$ (also the more general *map replacement technique*, as proposed in [Avrutin *et al.*, 2010], can be used, having the same purpose, and leading to the same results).

Once we have obtained the first two families of BCB curves of first complexity level (for example, given in (51) and (52)), considering two subsequent periodicity regions $\Pi_{\overline{L}\overline{R}^n}$ and $\Pi_{\overline{L}\overline{R}^{n+1}}$, the two subsequent BCB curves are given by $\Phi_{\overline{L}\overline{R}^n}$ and $\Phi_{\overline{R}\overline{L}\overline{R}^n}$, so that the map as in (33) can be considered defined via the two functions $\tilde{T}_{\overline{L}}$ and $\tilde{T}_{\overline{R}}$ as follows, $\tilde{T}_{\overline{L}}(x) = T_{\overline{R}}^n \circ T_{\overline{L}}(x)$ and $\tilde{T}_{\overline{R}}(x) = T_{\overline{R}}^n \circ T_{\overline{L}} \circ T_{\overline{R}}(x)$. That is:

$$x' = \overline{T}(x),$$
$$\overline{T}(x) = \begin{cases} \tilde{T}_{\overline{L}}(x) = \tilde{A}_l x + \tilde{B}_l & \text{if } x < d \\ \tilde{T}_{\overline{R}}(x) = \tilde{A}_r x + \tilde{B}_r & \text{if } x > d \end{cases} \tag{55}$$

where the coefficients are given by:

$$\tilde{A}_l = A_lA_r^n, \qquad \tilde{B}_l = A_r^nB_l + B_r\frac{(1-A_r^n)}{(1-A_r)}$$
$$\tilde{A}_r = A_lA_r^{n+1}, \quad \tilde{B}_r = A_r^nA_lB_r + \tilde{B}_l. \tag{56}$$

All the results of the BCB curves previously obtained can now be used, substituting the new coefficients $\tilde{A}_l$, $\tilde{B}_l$, $\tilde{A}_r$ and $\tilde{B}_r$ to the old ones A_l, B_l, A_r and B_r. This leads to two infinite families of BCB curves of second complexity level. For the periodicity regions $\Pi_{\overline{L}\overline{R}^n(\overline{L}\overline{R}^{n+1})^m}$ the boundary is given by the BCB curves $\Phi_{\overline{L}\overline{R}^n(\overline{R}\overline{L}\overline{R}^n)^m}$ and $\Phi_{(\overline{R}\overline{L}\overline{R}^n)\overline{L}\overline{R}^n(\overline{R}\overline{L}\overline{R}^n)^{m-1}}$ from (51) and (52):

$\Phi_{\overline{L}\overline{R}^n(\overline{R}\overline{L}\overline{R}^n)^m}$:

$$\tilde{B}_r = \frac{[d(1-\tilde{A}_l\tilde{A}_r^m) - \tilde{A}_r^m\tilde{B}_l](1-\tilde{A}_r)}{(1-\tilde{A}_r^m)} \tag{57}$$

$\Phi_{(\overline{R}\overline{L}\overline{R}^n)\overline{L}\overline{R}^n(\overline{R}\overline{L}\overline{R}^n)^{m-1}}$:

$$\tilde{B}_r = \frac{[d(1-\tilde{A}_l\tilde{A}_r^m) - \tilde{A}_r^{m-1}\tilde{B}_l](1-\tilde{A}_r)}{(1-\tilde{A}_r^{m-1}) + \tilde{A}_l\tilde{A}_r^{m-1}(1-\tilde{A}_r)} \tag{58}$$

and substituting in (57) the expressions given in (56) the BCBs of second level are obtained as a function of the parameters of the map in (33). Similarly, from (53) and (54) we can obtain the boundaries of the periodicity regions $\Pi_{\overline{L}\overline{R}^{n+1}(\overline{L}\overline{R}^n)^m}$ of the second infinite family. This mechanism can be repeated iteratively as a map of the coefficients.

4. Bifurcation Curves of the Map T

In this section, we consider the map T with two discontinuity points d_1 and d_2, with $d_1 < d_2$, and the other parameters as given in (2). In order to simplify our reasoning we shall consider this new discontinuity point d_1 as a parameter which is varied: it is decreased starting from d_2. When $d_1 = d_2$ the map T reduces to F, and the dynamics are known, as recalled in Sec. 2. Thus we consider $d_1 < d_2$, and assume that the second discontinuity point is fixed at $d_2 = \overline{d}_2$. We illustrate the bifurcation curves of the map T in the same figure, as shown in Fig. 2, for $d_1 < \overline{d}_2 = 1.8$. That is, the bifurcation curves of the map T as a function of the parameters d_1 and μ_R are those corresponding to the boundaries of the different colored regions in the left part of Fig. 2, i.e. the region characterized by $d_1 < \overline{d}_2 = 1.8$. In this case, among the parameters that are kept fixed and given in (3), there is also the value of the upper discontinuity point: $d_2 = \overline{d}_2 = 1.8$.

In order to obtain the analytical expressions of the bifurcation curves, we proceed by steps, analyzing different regions of the phase plane in Fig. 2(b) in the next subsections. First considering the periodicity regions connected with $\overline{d}_2 = 1.8$ (involving only two branches of function T), then considering the periodicity regions having triangular shape (involving three branches of T), and

finally the periodicity regions having quadrilateral shape (also involving three branches of T).

As the map T has two discontinuities, our notation must be extended in order to allow us to distinguish between BCBs caused by the collisions of a cycle with d_1 and with d_2. In the following, in the range $d_1 < d_2$ we shall use ϕ to denote BCB curves due to collision with d_1 while with ψ we denote those due to collision with d_2 (so that in this section the notation Φ refers to F whereas ϕ and ψ refer to T).

4.1. *Periodicity regions associated with L and R branches only*

Let us start describing what occurs to the bifurcation curves already existing for the map with only one discontinuity point (i.e. map F and the related bifurcation curves shown in Fig. 2 for $d_2 > 1.8$) when a new discontinuity is introduced in $d_1 < d_2$. When $d_1$is close enough to d_2, all the periodicity regions associated with the cycles existing for F also exist for T, but keeping fixed $\overline{d}_2$ their boundaries are changed. Even if a third branch of the map is introduced, the cycles of the map T associated with the periodicity regions coming from those of the map F are such that the related cycles have periodic points belonging only to the first and third branches (denoted by the letters L and R respectively), i.e. the cycle has no periodic points in the middle region (denoted by M). This case is clearly simple to analyze. The example associated with a 3-cycle LR^2 is shown in Fig. 6. Therefore, the BCBs of a cycle associated with the symbolic sequence LR^n occur due to the collision of the periodic point in L with the discontinuity point d_1 and by the collision of the smallest point in R with the discontinuity point d_2. Hence, the upper boundary of its existence region is the same curve that we have already calculated in Sec. 2. The equation of this BCB is given by (13), which we rewrite for convenience, because now it is a function of the discontinuity point d_1 (and not of d_2):

$$\phi_{LR^n} : \mu_R = \frac{[d_1(1 - a_L a_R^n) - a_R^n \mu_L](1 - a_R)}{(1 - a_R^n)}. \tag{59}$$

For $n = 2$ we have the upper boundary of the region Π_{LR^2} of the 3-cycle in Fig. 7 [the shape of the map at this BCB is shown in Fig. 6(a)].

We know that for the map F the region of existence for $d_2 > \overline{d}_2 = 1.8$ closes when the last periodic point x_n^* in the R side reaches the discontinuity point d_2, and its equation $\Phi_{RLR^{n-1}}$ is given by (14). Also now, for the map T in (1), the BCB giving the boundary of the existence region (i.e. border collision causing the disappearance of the cycle) occurs when the last periodic point of the cycle in the R side reaches the discontinuity point $\overline{d}_2$ [Fig. 6(b) shows this BCB for the 3-cycle]. That is, the lower boundaries of such a periodicity region in the parameter plane (d_1, μ_R) are the same curves that we have already found for the map (4), with the fixed value for d_2, i.e. $d_2 = \overline{d}_2$ ($\overline{d}_2 = 1.8$ in our examples):

$$\psi_{RLR^{n-1}} : \mu_R = \frac{[\overline{d}_2(1 - a_L a_R^n) - a_R^{n-1} \mu_L](1 - a_R)}{(1 - a_R^{n-1}) + a_L a_R^{n-1}(1 - a_R)}. \tag{60}$$

This curve is a horizontal straight line in the parameter plane (d_1, μ_R). The shape of the map T when the parameters are in the upper and the lower points of the region of the 3-cycle crossed by the vertical hatched line in Fig. 7(b), for $d_1 < \overline{d}_2$, are shown in Figs. 6(a) and 6(b), respectively.

The periodicity regions in the parameter plane (d_1, μ_R) bounded by the curves whose equations are given above, in (59) and (60), exist up to their intersection. In the case of the periodicity regions of

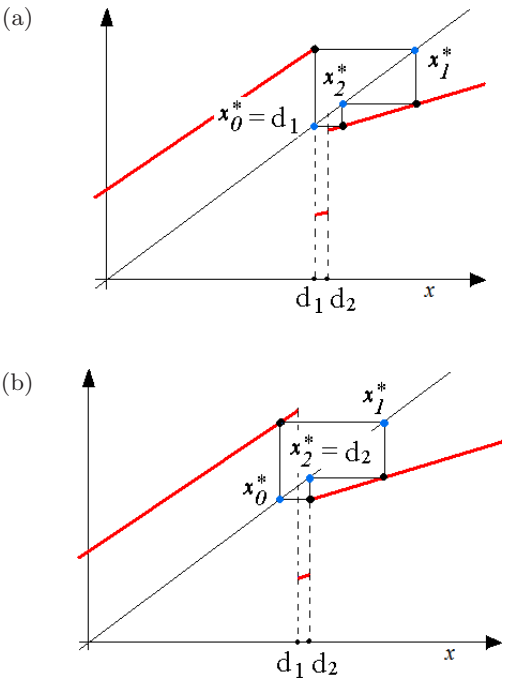

Fig. 6. BCB of a 3-cycle. (a) BCB due to the merging of x_0^* with d_1. (b) BCB due to the merging of x_2^* with d_2.

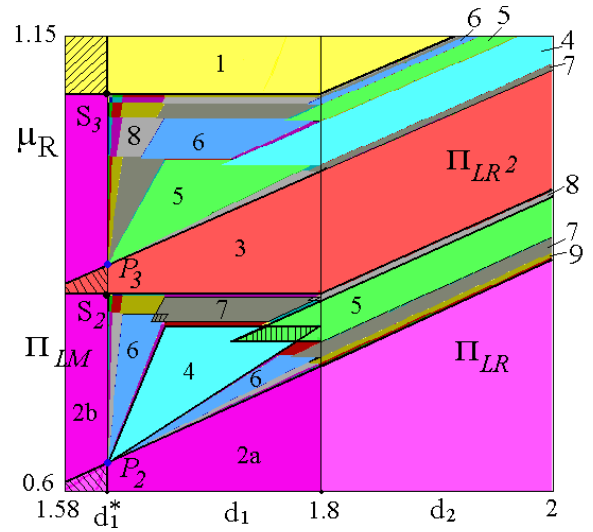

(a)

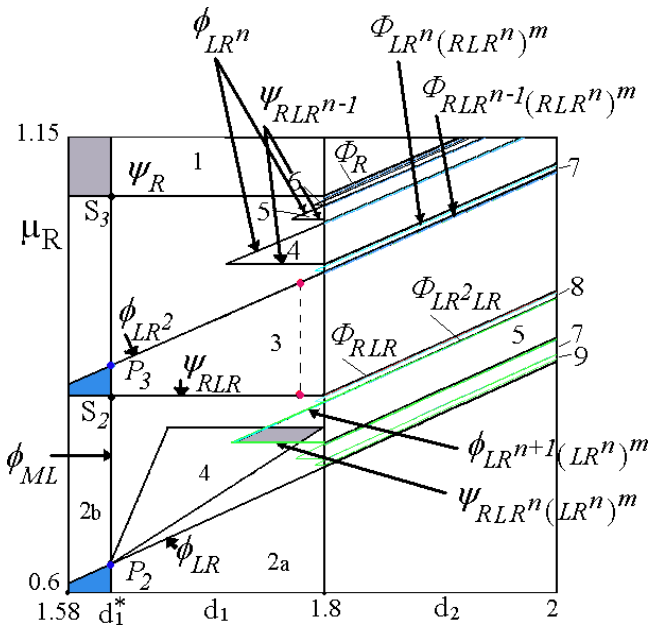

(b)

Fig. 7. Enlarged part of Fig. 1, with BCB curves obtained analytically in (b).

first level of complexity given above, the intersection point between the upper and the lower boundaries can be calculated using Eqs. (59) and (60) and is given by:

$$d_1 = \frac{a_R^n \mu_L}{(1 - a_L a_R^n)} + \frac{[\bar{d}_2(1 - a_L a_R^n) - a_R^{n-1}\mu_L](1 - a_R^n)}{[(1 - a_R^{n-1}) + a_L a_R^{n-1}(1 - a_R)](1 - a_L a_R^n)}. \quad (61)$$

For $n = 2, 3, \ldots$, i.e. for the periods $3, 4, 5, \ldots$ see the main regions in Fig. 7.

What we have explained above (the equations of the BCB curves of the first level of complexity) also holds for all the regions of any level of complexity existing on the right side of $\bar{d}_2$ for the map F. For example, the periodicity regions associated with cycles of the second level of complexity computed in Sec. 2 in (26) and (27) are used to obtain the BCB curves of T. So the upper boundary is given by the following BCB curves:

$\phi_{LR^n(RLR^n)^m}$:

$$\mu_R = d_1(1 - a_R) + \frac{d_1(1 - a_L) - \mu_L}{\dfrac{a_L H'}{1 + H'} + \dfrac{1 - a_R^n}{(1 - a_R)a_R^n}} \quad (62)$$

and the lower horizontal line by:

$\psi_{RLR^{n-1}(RLR^n)^m}$:

$$\mu_R = \bar{d}_2(1 - a_R) + \frac{\bar{d}_2(1 - a_L) - \mu_L}{\dfrac{a_L H''}{1 + H''} + \dfrac{1 - a_R^n}{(1 - a_R)a_R^n}} \quad (63)$$

so that their intersection point is obtained when d_1 satisfies the following equation:

$$d_1(1 - a_R) + \frac{d_1(1 - a_L) - \mu_L}{\dfrac{a_L H'}{1 + H'} + \dfrac{1 - a_R^n}{(1 - a_R)a_R^n}} = \bar{d}_2(1 - a_R) + \frac{\bar{d}_2(1 - a_L) - \mu_L}{\dfrac{a_L H''}{1 + H''} + \dfrac{1 - a_R^n}{(1 - a_R)a_R^n}}. \quad (64)$$

Also for the other pairs of regions of the second level of complexity [from Eqs. (29) and (30)] we have now regions with the upper boundary given by

$\phi_{LR^{n+1}(LR^n)^m}$:

$$\mu_R = d_1(1 - a_R) + \frac{d_1(1 - a_L) - \mu_L}{\dfrac{a_L}{1 + S'} + \dfrac{1 - a_R^n}{(1 - a_R)a_R^n}} \quad (65)$$

and the lower horizontal line by

$\psi_{RLR^n(LR^n)^m}$:

$$\mu_R = \bar{d}_2(1 - a_R) + \frac{\bar{d}_2(1 - a_L) - \mu_L}{\dfrac{a_L}{1 + S''} + \dfrac{1 - a_R^n}{(1 - a_R)a_R^n}} \quad (66)$$

so that their intersection point is obtained when d_1 satisfies the following equation:

$$d_1(1-a_R)+\frac{d_1(1-a_L)-\mu_L}{\dfrac{a_L}{1+S'}+\dfrac{1-a_R^n}{(1-a_R)a_R^n}} = \bar{d}_2(1-a_R)+\frac{\bar{d}_2(1-a_L)-\mu_L}{\dfrac{a_L}{1+S''}+\dfrac{1-a_R^n}{(1-a_R)a_R^n}}. \quad (67)$$

Some of these regions of second level of complexity are drawn, in color, in Fig. 7(b). Similarly we can reason for all the other bifurcation curves of the map T, involving only the L and R branches.

Summarizing: *All periodicity regions existing for the map F also exist for the map T in a suitable region of the complete parameter space and, as we will see below, the related cycle may be the unique one for T, or it may coexist with another cycle whose periodic points also involve the middle branch M. The periodicity regions of these cycles are, in our figures, all those starting in the range $d_2 > \bar{d}_2$ and entering in the range $d_1 < \bar{d}_2$ with a horizontal line as lower boundary.*

4.2. *Coexistence*

As already mentioned in the Introduction, with two discontinuity points, our map may have coexisting cycles. The discontinuity points behave as critical points in the smooth case, and each discontinuity point may be associated with at least one attracting set. In the cases considered in this paper, with positive slopes and smaller than 1 (which implies that the invariant sets may only be attracting cycles or an invariant Cantor set), each discontinuity point may be associated with only one attracting cycle. In fact, it is known that two different attracting cycles may be associated with the two extrema at one discontinuity point only when the two branches of the map are one increasing and one decreasing (see [Avrutin & Schanz, 2006; Avrutin *et al.*, 2006; Gardini & Tramontana, 2010]). Thus in the parameter regions considered in this paper, the map T can have at most two coexisting cycles. A few hatched regions, which are the simplest cases of coexistence, are clearly shown in Fig. 7(a), and we can see that there exist several other overlapping regions, associated with the coexistence of two different cycles of T.

The coexistence for itself is not so unexpected. However, the overlapping of two regions leads, in the parameter space, to the intersection of two different BCB curves. On each curve, a periodic point of a cycle collides with one discontinuity point. Thus at each crossing point we have only two possibilities:

(j) either the two cycles of T are colliding with the same discontinuity point, or
(jj) one cycle of T collides with d_1 and the other with d_2.

In the case (j) the intersection point is a big-bang bifurcation point at which Theorem 1 can be applied. Thus a complete set of periodicity regions issues from such a point, and knowing the sequences of the colliding cycles we are able to predict the sequences of everything that emerges there. The bifurcation points denoted as P_2 and P_3 in Fig. 7 are of such kind.

In the case (jj) the intersection point plays a different role. No periodicity region issues from it. However, an intersection of two BCB curves leads to four regions: one of overlapping (associated with the coexistence of the two cycles), two regions of single existence, and one region in which both cycles do not exist. In our case (where repelling cycles cannot exist) this region clearly cannot be empty. The two regions of single existence have one side which is the limit set of infinitely many BCB curves. Thus their intersection leads to a new kind of bifurcation point, limit sets of a doubly infinite sequence of other periodicity regions. This bifurcation point (at which two cycles collide) is a limit set of a doubly infinite sequence of BCB curves. The points denoted as S_2 and S_3 in Fig. 7 are of this kind, as well as all the points associated with the other overlapping regions shown in Fig. 7, except for P_2 and P_3.

Let us now start with the simplest cycles. The lower region of the 2-cycle called 2a in Fig. 7(a) refers to the 2-cycle with periodic points in the L and R branches. This region is bounded by the bifurcation curve described in the previous subsection: it is given by the upper boundary of the region of the first level of complexity obtained from the curve in (59) with $n = 1$, that is, the straight line

$$\phi_{LR}: \mu_R = d_1(1-a_La_R)-a_R\mu_L \quad \text{for } d_1 < \bar{d}_2. \quad (68)$$

The upper region [with the number 1 in Fig. 7(a)] is the region of stability of the fixed point $P_R^* = \frac{\mu_R}{1-a_R}$ of the right branch. Its region in the parameter plane (d_2, μ_R) is bounded below by the straight line

$$\Phi_R : \mu_R = d_2(1 - a_R) \quad \text{for } d_2 > \bar{d}_2 \tag{69}$$

and by the horizontal line

$$\psi_R : \mu_R = \bar{d}_2(1 - a_R) \quad \text{for } d_1 < \bar{d}_2 \tag{70}$$

in the parameter plane (d_1, μ_R).

In Fig. 7(a) we also see another region associated with a 2-cycle, called 2b, which is related with periodic points to the two branches L and M. From the condition $x = f_M \circ f_L(x) = a_M(a_L x + \mu_L) + \mu_M$, we have the periodic points of this 2-cycle, that is:

$$\begin{aligned} x_L^* &= \frac{a_M\mu_L + \mu_M}{1 - a_L a_M}, \\ x_M^* &= f_L(x_L^*) = a_L \frac{a_M\mu_L + \mu_M}{1 - a_L a_M} + \mu_L \end{aligned} \tag{71}$$

and it exists when $x_L^* < d_1$ and $d_1 < x_M^*$ (and clearly also $x_M^* < d_2$). It follows that one boundary of the existing region of this 2b-cycle is given by $x_M^* = d_1$, that is,

$$\phi_{ML} : d_1 = d_1^*, \quad d_1^* = a_L \frac{a_M\mu_L + \mu_M}{1 - a_L a_M} + \mu_L \tag{72}$$

[the vertical line in Fig. 7(a) at $d_1 = d_1^* \simeq 1.61644$, as it is independent of μ_R], and the other boundary is given by $x_L^* = d_1$, that is

$$\phi_{LM} : d_1 = \frac{a_M\mu_L + \mu_M}{1 - a_L a_M} \tag{73}$$

(which is not in the parameter range of our figure).

As it is easy to see in Fig. 7(a), the vertical strip of the 2b-cycle intersects the regions of several other coexisting cycles (hatched regions): the fixed point, the 3-cycle of first level of complexity, the 2a-cycle of first level of complexity, and more intersections exist for lower values of the parameter μ_R [with all the families of the first level of complexity below the 2a-cycle as shown in Fig. 2(a)].

In Fig. 7(b) the point P_2 given by the intersection between ϕ_{ML} and ϕ_{LR} satisfies the assumptions of Theorem 1 at the discontinuity point $x = d_1$. In fact, the periodic point of the 2-cycle 2a is collides from the left side of d_1 while the periodic point x_M^* of the 2-cycle 2b is collides from the right side of d_1. Thus we know that from this bifurcation point, a set of infinitely many other BCB curves will emerge, in a proper adding structure, and the related starting sequences in order to apply Theorem 1 are $\overline{L} = LR$ and $\overline{R} = ML$ (which we shall use in the next subsection).

Similarly the point P_3 given by the intersection between ϕ_{ML} and ϕ_{LRR} satisfies the assumptions of the theorem at the discontinuity point $x = d_1$. In fact, the periodic point of the 3-cycle of T having symbolic sequence RLR is collides from the left side of d_1 while the periodic point x_M^* of the 2-cycle 2b is collides from the right side of d_1. So the related starting sequences in order to apply Theorem 1 are $\overline{L} = LRR$ and $\overline{R} = ML$.

The intersection of the bifurcation curve ϕ_{ML} with the BCB curves ψ_R given above and ψ_{RLR} (given in (60) for $n = 2$) leads to the points S_2 and S_3, respectively.

Besides the overlapping regions associated with the coexistence with the 2b-cycle, it is clear that infinitely many regions of coexistence exist in the strip bounded by the vertical lines $d_1 = d_1^* \simeq 1.61644$ and $d_1 = \bar{d}_2 = 1.8$. This region in the middle is associated with cycles having periodic points also in the middle branch M, and we have infinitely many overlappings in regions both with triangular and quadrilateral shapes, a few of which are shown in Fig. 7.

As we have seen, all the BCB curves in the strip $(d_1^*, \bar{d}_2)$ issuing from $\bar{d}_2$ are of triangular shape and a portion is overlapped with different triangular regions issuing from P_2. For example, in Fig. 7(b) see the overlapping between the region of a 4-cycle, involving periodic points in the L and M branches, and the region of a 5-cycle, involving periodic points in the branches L and R. As we shall see below, all the BCB curves in the strip $(d_1^*, \bar{d}_2)$ issuing from P_2 are of triangular shape and one corner is overlapped with different other regions: the fan on the right side of the periodicity region of the 4-cycle with regions coming from $\bar{d}_2$, while the fan of triangular shape on the left side of the same region has a corner overlapped with periodicity regions having quadrilateral shape. All the periodicity regions of quadrilateral shape have two opposite corners which overlap with two other different regions. See, as an example, the period 7 region shown in Fig. 7(a) in the middle region. These periodicity regions will be explained in the following subsections.

4.3. *Periodicity regions issuing from P_2*

We can see the parameter region in the strip $(d_1^*, \bar{d}_2)$ as the interaction of two maps having both one discontinuity point (in different places). That is, as we have seen above, when the parameter d_1 is far from $\bar{d}_2$ (for $d_1 < d_1^*$, as defined in (72)) we have cycles associated only with the first two branches of the map, i.e. with $f_L(x)$ and $f_M(x)$ and the discontinuity d_1. When no periodic point belongs to the branch R then we exactly have the dynamics associated with a map having only one discontinuity point. In this case, with the obvious changes in the parameters, we can repeat all what we have described in Sec. 2 for the map with only one discontinuity (clearly using the branches L and M instead of L and R and discontinuity point d_1 instead of d_2). By contrast, when the parameter d_1 is between d_1^* and $\bar{d}_2$, then we are in a parameter region truly new, where, apart from the cycles already described in Sec. 4.1, the cycles have periodic points in all the three branches of T.

Here we shall characterize the BCB issuing from the intersection points of two different BCB curves, as the point P_2 already described in Sec. 4.2. Clearly we can reason similarly for the intersection point P_3, and for the infinitely many similar points existing at lower values of μ_R, as shown in Fig. 2(a).

As already remarked, considering the bifurcation point P_2, given [from the intersection of ϕ_{ML} and ϕ_{LR} in Eqs. (68) and (72)] by:

$$\begin{aligned} P_2 &= (d_1^*, d_1^*(1 - a_L a_R) - a_R \mu_L), \\ d_1^* &= a_L \frac{a_M \mu_L + \mu_M}{1 - a_L a_M} + \mu_L \end{aligned} \tag{74}$$

we are in the proper situation to apply the adding scheme described in Sec. 3, and the related starting sequences are $\overline{L} = LR$ and $\overline{R} = ML$.

As an example, in Fig. 8 we show the bifurcation occurring when a parameter point crosses from the region of bistability through P_2 to the right side, where the 2-cycles do not exist. Consider the regions Π_{LR} and Π_{ML}. Taking a point in the overlapping region, then the two 2-cycles coexist, as shown in Fig. 8(a). The 2a-cycle has periodic points $\{y_L^*, y_R^*\}$, while the 2b-cycle has periodic points $\{x_L^*, x_M^*\}$ with $x_L^* < y_L^*$. Their basins are separated by the two discontinuity points d_1 and d_2 and their preimages. If the parameters are changed so that (d_1, μ_R) belongs to the opposite side of the crossing, where both the 2-cycles do not exist, then, as we know from Sec. 3, infinitely many distinct periodicity regions exist. In Fig. 8(b) we show an example with an attracting 4-cycle (which is the main periodicity region between ϕ_{ML} and ϕ_{LR}).

In order to determine the two lateral boundaries of the BCB curves of the periodicity regions issuing from P_2 and having a triangular shape, we follow the steps described in Sec. 3. Considering as $\Phi_{\overline{L}}$ the BCB curve ϕ_{LR} and as $\Phi_{\overline{R}}$ the BCB curve ϕ_{ML}, we can use the map defined in (33) with the

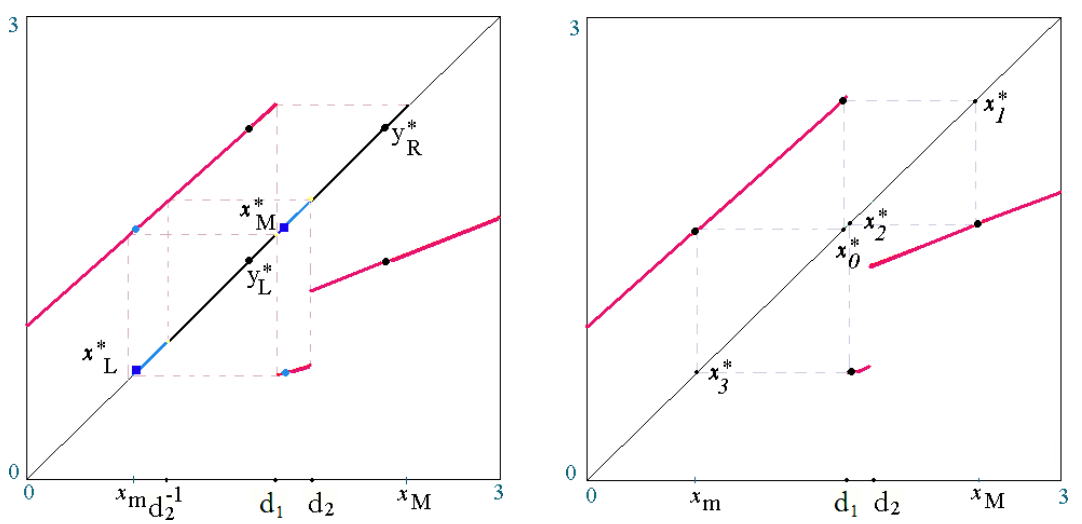

Fig. 8. (a) Two coexisting cycles of period 2, at the parameters' values given in (3) and $\mu_R = 0.5$, $d_1 = 1.585$, $d_2 = 1.8$. (b) A unique 4-cycle existing at $\mu_R = 0.67$, $d_1 = 1.65$, $d_2 = 1.8$.

composite functions $T_{\overline{L}}$ and $T_{\overline{R}}$ given by

$$T_{\overline{L}}(x) = f_R \circ f_L(x) = A_l x + B_l, \quad A_l = a_L a_R, \quad B_l = a_R \mu_L + \mu_R \tag{75}$$

$$T_{\overline{R}}(x) = f_L \circ f_M(x) = A_r x + B_r, \quad A_r = a_L a_M, \quad B_r = a_L \mu_M + \mu_L. \tag{76}$$

Then, all the infinite families (of first level of complexity) of periodicity regions of cycles having the symbolic sequence $\overline{L}\overline{R}^m$ and $\overline{R}\overline{L}^m$ for any $m \geq 1$ lead to a fan of regions issuing from P_2, between the two starting BCB curves ϕ_{LR} and ϕ_{ML}.

Let us first consider the family $\overline{L}\overline{R}^m$ which is involved in periodicity regions having as limit set the BCB curve ϕ_{ML}. In order to determine the BCB curves on the two boundaries of these regions, we can use Eqs. (51) and (52), with $d = d_1$, and the parameters A_l, B_l, A_r and B_r defined in (75) and (76), respectively. Then, rearranging, we obtain:

$\phi_{(LR)(ML)^m}$:

$$\mu_R = \frac{d_1(1 - A_l A_r^m)}{A_r^m} - \frac{B_r(1 - A_r^m)}{A_r^m(1 - A_r)} - a_R \mu_L$$

$\phi_{(ML)(LR)(ML)^{m-1}}$:

$$\mu_R = \frac{d_1(1 - A_l A_r^m)}{A_r^{m-1}} - \frac{B_r[(1 - A_r^{m-1}) + A_l A_r^{m-1}(1 - A_r)]}{A_r^{m-1}(1 - A_r)} - a_R \mu_L.$$

The bifurcation curves $\phi_{(LR)(ML)^m}$ give the straight lines representing the *left boundaries* of the periodicity regions of the cycles of period $k = 2 + 2m = 2(1 + m)$ which have the BCB curve ϕ_{ML} as limit set, as shown in Fig. 9(b) for $m = 1, 2, 3$. The curves $\phi_{(ML)(LR)(ML)^{m-1}}$ represent the *right boundaries* of these periodicity regions.

Now consider the other family of cycles with symbolic sequence $\overline{R}\overline{L}^m$, from Eqs. (53) and (54), with $d = d_1$, and the parameters A_l, B_l, A_r and B_r defined in (75) and (76), respectively, we obtain:

$\phi_{(ML)(LR)^m}$:

$$\mu_R = \frac{[d_1(1 - A_r A_l^m) - A_l^m B_r](1 - A_l)}{(1 - A_l^m)} - a_R \mu_L \tag{77}$$

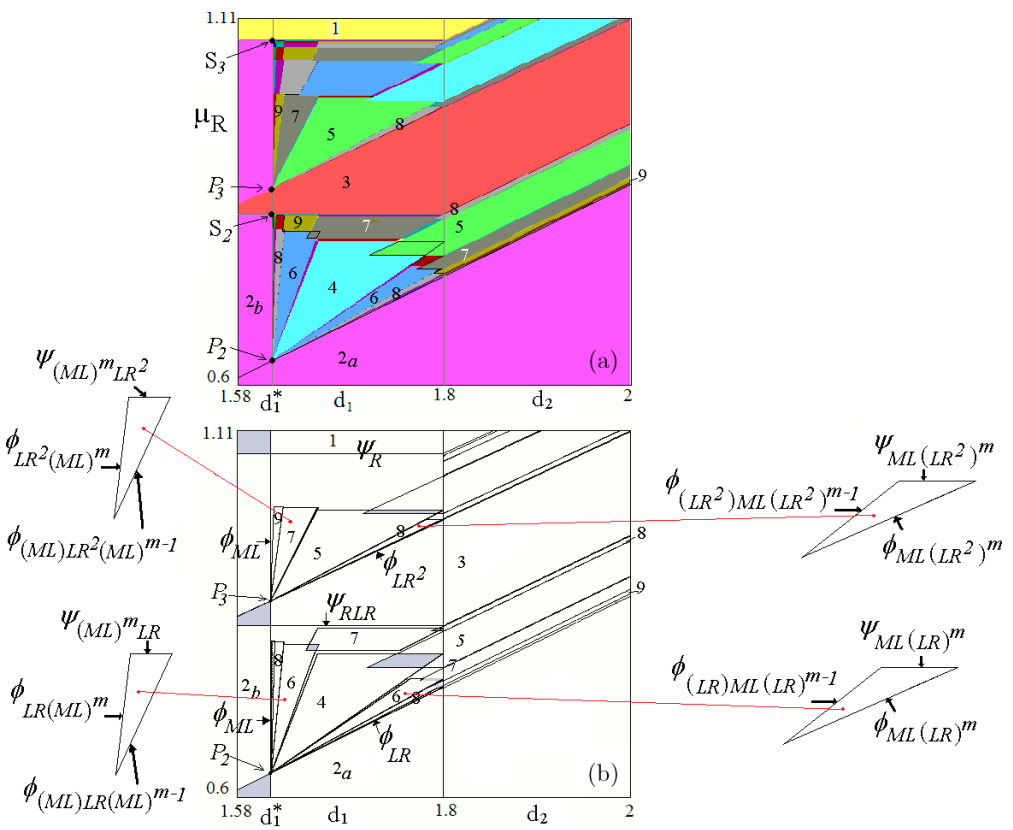

Fig. 9. Enlarged part of Fig. 1, with BCB curves obtained analytically in (b).

and:

$$\phi_{(LR)(ML)(LR)^{m-1}}:$$

$$\mu_R = \frac{[d_1(1-A_rA_l^m) - A_l^{m-1}B_r](1-A_l)}{(1-A_l^{m-1}) + A_rA_l^{m-1}(1-A_l)} - a_R\mu_L. \quad (78)$$

These bifurcation curves represent the straight lines which bound the periodicity regions of the cycles of period $k = 2(1+m)$ which have the BCB curve ϕ_{LR} (upper boundary of the region of the 2a-cycle) as limit set. A few of them are shown in Fig. 9(b).

Up to now, we have obtained both the lateral boundaries of these periodicity regions, but we still miss their *upper boundaries*. To calculate these boundaries we have to note that a periodic point belonging to the branch M may collide not only with the discontinuity in d_1 but also with d_2.

Considering the family of cycles with symbolic sequence $\overline{R}\overline{L}^m$, i.e. $(ML)(LR)^m$, the straight lines, defined above as lower boundaries, all intersect the vertical line $d = \overline{d}_2$, which means that the periodic point in the region M (which, in this family, is a unique point) collides with d_2, thus the upper boundaries of these periodicity regions are horizontal straight lines of equation as in $\phi_{(ML)(LR)^m}$ but with d_1 replaced by $\overline{d}_2$. Therefore, we obtain for these boundaries, the BCB curves:

$$\psi_{(ML)(LR)^m}:$$

$$\mu_R = \frac{[\overline{d}_2(1-A_rA_l^m) - A_l^mB_r](1-A_l)}{(1-A_l^m)} - a_R\mu_L. \quad (79)$$

Let us now turn to the upper boundaries of the family of cycles with symbolic sequence $\overline{L}\overline{R}^m = (LR)(ML)^m$. In this case, the BCB occurs due to the collision of the periodic point of the cycle belonging to the branch M closest to d_2, colliding with d_2. This colliding periodic point is the fixed point of the function $T_{\overline{L}} \circ T_{\overline{R}}^m(x)$. Then from $T_{\overline{R}}^m(x) = A_r^m x + B_r\frac{(1-A_r^m)}{(1-A_r)}$ we have

$$T_{\overline{L}} \circ T_{\overline{R}}^m(x) = A_l\left(A_r^m x + B_r\frac{(1-A_r^m)}{(1-A_r)}\right) + B_l. \quad (80)$$

The solution of $T_{\overline{R}}^m \circ T_{\overline{L}}(x) = x$ satisfies

$$x(1-A_r^mA_l) = A_lB_r\frac{(1-A_r^m)}{(1-A_r)} + B_l \quad (81)$$

and the corresponding BCB curves are given by:

$$\overline{d}_2(1-A_r^mA_l) = A_lB_r\frac{(1-A_r^m)}{(1-A_r)} + B_l \quad (82)$$

therefore we obtain:

$$\psi_{(ML)^m(LR)}:$$

$$\mu_R = \overline{d}_2(1-A_r^mA_l) - A_lB_r\frac{(1-A_r^m)}{(1-A_r)} - a_R\mu_L. \quad (83)$$

Clearly the intersection of the lines so defined with the BCB curves $\phi_{(ML)(LR)(ML)^{m-1}}$ completely defines these periodicity regions having a triangular shape.

We have this completely described the boundaries of two infinite families of periodicity regions of the first complexity level issuing from point P_2. The boundaries of the regions which belong to higher levels of complexity can be similarly calculated.

A similar reasoning leads to the families of BCB curves issuing from point P_3, given by the intersection of the BCB curves ϕ_{LR^2} [from (59) for $n = 2$] and ϕ_{ML} [given in (72)], so, in the parameter plane (d_1, μ_R), we have

$$P_3 = \left(d_1^*, \frac{d_1^*(1-a_La_R^2) - a_R^2\mu_L}{(1+a_R)}\right), \quad d_1^* = a_L\frac{a_M\mu_L + \mu_M}{1-a_La_M} + \mu_L. \quad (84)$$

We can apply the steps described in Sec. 3, with starting sequences $\overline{L} = LRR$ and $\overline{R} = ML$. Then, considering as $\Phi_{\overline{L}}$ the BCB curve ϕ_{LRR} and as $\Phi_{\overline{R}}$ the BCB curve ϕ_{ML}, we can use the map defined in (33) with the composite functions $T_{\overline{L}}$ and $T_{\overline{R}}$ given by:

$$T_{\overline{L}}(x) = f_R^2 \circ f_L(x) = A_lx + B_l, \quad A_l = a_La_R^2, \quad B_l = \mu_La_R^2 + a_R\mu_R + \mu_R \quad (85)$$

$$T_{\overline{R}}(x) = f_L \circ f_M(x) = A_rx + B_r, \quad A_r = a_La_M, \quad B_r = a_L\mu_M + \mu_L. \quad (86)$$

Then we can proceed iteratively, by using the same formulas given in Sec. 3 with the new aggregate parameters defined in (85) and (86). In Fig. 9 we have shown a few BCB curves of the families $\Phi_{\overline{L}\overline{R}^m} = \phi_{(LR^2)(ML)^m}$ (*left boundaries* of the periodicity regions, having as limit set the BCB ϕ_{ML}) and $\Phi_{\overline{R}\overline{L}\overline{R}^{m-1}} = \phi_{(ML)(LR^2)(ML)^{m-1}}$ (*right boundaries*) of

the first level of complexity, as well as of $\Phi_{\overline{R}\overline{L}^m} = \phi_{(ML)(LR^2)^m}$ and $\Phi_{\overline{L}\overline{R}\overline{L}^{m-1}} = \phi_{(LR^2)(ML)(LR^2)^{m-1}}$.

We remark that all the periodicity regions issuing from P_2 located on the right of the region Π_{MLLR}, associated with the 4-cycle in the middle, have a corner point on the line $d_2 = \overline{d}_2$. Thus all have a point in common with some periodicity region existing on the right of this point, for the map F, and belonging to a bistability region. The situation for point P_3 is similar.

All the periodicity regions of the families issuing from P_2 are below the boundary of the BCB curve ψ_{RLR}. Similarly for P_3, the upper boundary is the BCB curve of the fixed point ψ_R.

Therefore, there are empty spaces in the parameter region, which must be necessarily filled with other periodicity regions. These regions have quadrilateral shapes and are described in the next subsection.

4.4. *Quadrilateral periodicity regions*

Let us first remark that in the case of our map T, with two discontinuity points, any periodicity region cannot have more than four boundaries. In fact, a periodicity region refers to a unique cycle, and it can appear/disappear only via collision of a periodic point with the border of definition of the functions. So a periodic point may collide with d_1 from the right or left side, and may collide with d_2 from the right or left side. Thus *the existence region of a cycle can have at most four BCB curves.*

In the part of the parameter space that we are considering, there also are regions with quadrilateral shapes. An example for such a region (with period 7) is shown in Fig. 10.

In Theorem 1 proved in Sec. 3 we have described infinite families issuing from a big-bang

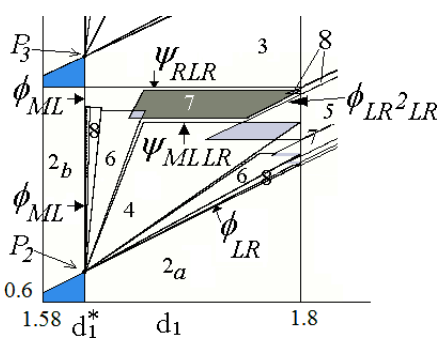

Fig. 10. Quadrilateral periodicity region Π_7.

bifurcation point, intersection of two BCB curves. However, the quadrilateral regions are seemingly not originating from such a point. To explain the BCB curves bounding these regions we have to recall that the overall parameter space of the system we are investigating is eight-dimensional and the bifurcation structure we can observe in our figures represents only a two-dimensional cut across some structure in this eight-dimensional space. Therefore we can assume that at some place in this parameter space the BCB curve ϕ_{ML}, located in our figures on the left side of the region with period 7 (a collision from M side with d_1) intersects the curve ϕ_{LR^2LR}, located on the right side of this region (a collision from L side with d_1). Then, from this intersection point the complete period adding structure must originate. Depending on their size (in the eight-dimensional parameter space) some regions issuing from this intersection point may reach the two-dimensional parameter subspace that we are investigating. Especially, considering as starting sequences $\overline{R} = ML$ and $\overline{L} = LR^2LR$, we can define the composite functions

$$\begin{aligned} T_{\overline{L}}(x) &=: f_R \circ f_L \circ f_R \circ f_R \circ f_L(x) \\ T_{\overline{R}}(x) &=: f_L \circ f_M(x) \end{aligned} \tag{87}$$

for the calculation of the BCB curves defining the boundaries of periodicity regions for two infinite families of cycles of the first complexity level. Then, using Eqs. (51) and (52) we calculate the BCB curves of cycles with symbolic sequence $\overline{L}\overline{R}^m$ and $\overline{R}\overline{L}\overline{R}^{m-1}$, which give the BCB curves

$$\phi_{(LR^2LR)(ML)^m}, \quad \phi_{(ML)(LR^2LR)(ML)^{m-1}} \tag{88}$$

defining the boundaries of the periodicity regions forming the first family (for $m \to \infty$ these curves accumulate to the BCB curve $\overline{R}$, i.e. ϕ_{ML}). Similarly, using Eqs. (53) and (54) we calculate the BCB curves

$$\phi_{(LR^2LR)(ML)(LR^2LR)^{m-1}}, \quad \phi_{(ML)(LR^2LR)^m} \tag{89}$$

which define the boundaries of the periodicity regions forming the second family, accumulating for $m \to \infty$ to the BCB curve ϕ_{LR^2LR}. Note also that the 7-cycle mentioned above belongs to both these families for $m = 1$. A few periodicity regions bounded by the curves in (88) and (89) are shown in Fig. 11.

So far we have determined two boundaries of each region belonging to the two families mentioned above. Now the question arises which BCB curves

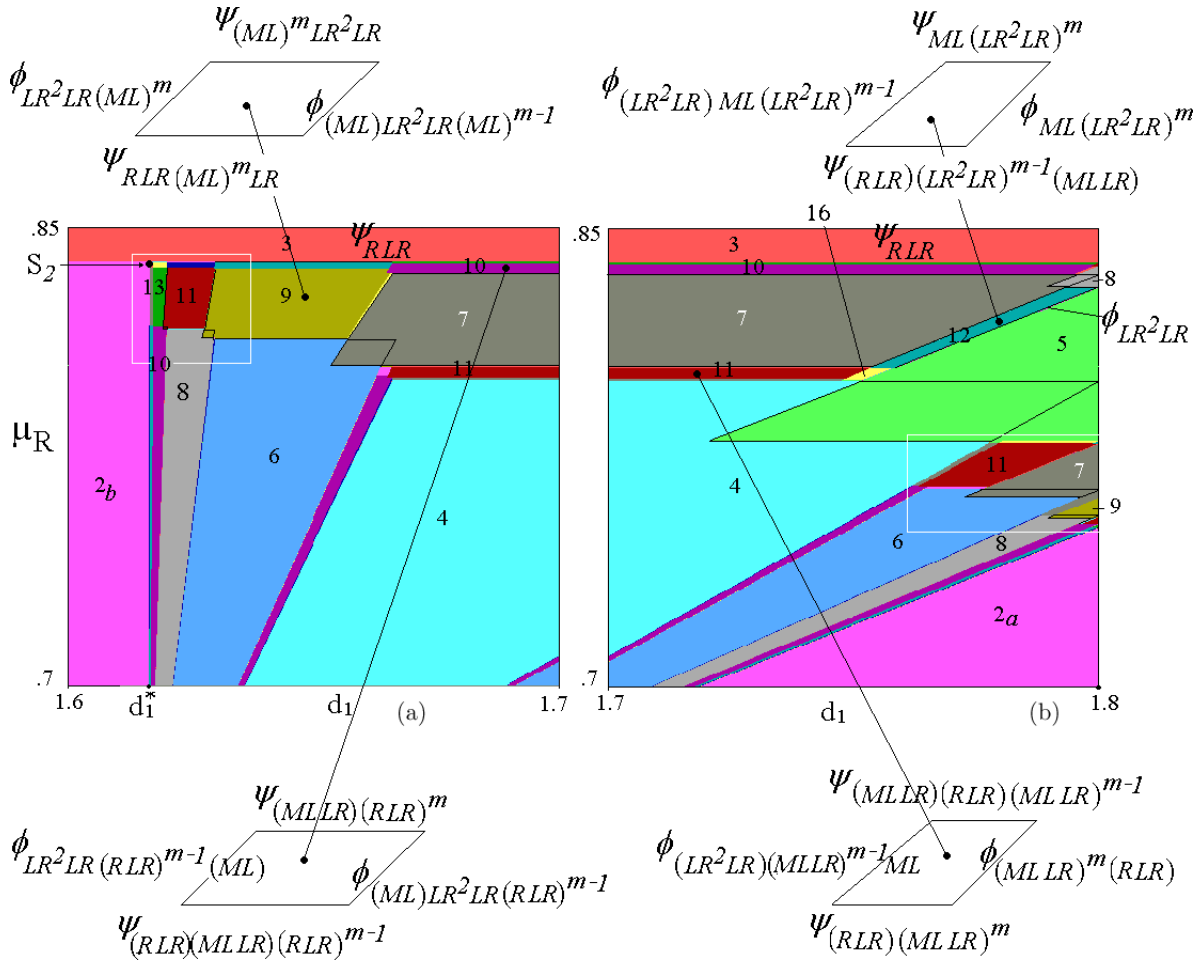

Fig. 11. Enlarged portions of Fig. 9(a).

define the two other boundaries of each of these regions. Clearly, when dealing with these bifurcations, the symbolic sequences we determined so far must remain the same (since they are associated with the same cycles), but cyclically shifted in a different way. Moreover, as we already mentioned above, for each cycle there are only two points which can collide with each discontinuity. Therefore, the two other BCB curves *must* be caused by collisions of some points of the cycles with the other discontinuity, that means with d_2.

To determine the equations of the upper and lower boundaries of the quadrilateral regions located on the left of Π_7, we have to note that these regions are located below the BCB curve of the 3-cycle ψ_{RLR} (where a collision with d_2 from R side occurs) and above the fan of regions with the first complexity level issuing from P_2, whose upper boundaries are the BCB curves $\psi_{(ML)^m(LR)}$ (where a collision with d_2 from M side occurs). Hence, we can assume that somewhere in the eight-dimensional parameter space these bifurcations curves intersect and the situation at the intersection point fulfills the conditions of Theorem 1. Then we define the composite map using

$$\begin{aligned} T_{\overline{L}}(x) &=: f_R \circ f_L \circ (f_L \circ f_M)^m(x) \\ T_{\overline{R}}(x) &=: f_R \circ f_L \circ f_R(x) \end{aligned} \tag{90}$$

that is, assuming $\overline{L} = (ML)^m(LR)$ and $\overline{R} = RLR$, we calculate the BCB curves with symbolic sequence $\overline{L}\overline{R}$ i.e. $(ML)^m(LRRLR)$ for the upper boundaries and $\overline{R}\overline{L}$ i.e. $(RLR)(ML)^m(LR)$ for the lower boundaries thus obtaining the BCB curves

$$\psi_{(ML)^m LR(RLR)}, \quad \psi_{(RLR)(ML)^m LR} \tag{91}$$

completing the description of the quadrilateral regions on the left of Π_7 [see also Fig. 11(a)].

The next upper/lower boundaries we explain is for the family located on right of Π_7 [see Fig. 11(b)].

We can see that (as for the considered boundary of the 5-cycle) all of them reach the discontinuity point colliding with d_2, thus the *upper boundaries* of these periodicity regions are horizontal straight lines of equation as in $\phi_{(ML)(LR^2LR)^m}$ but with d_1 replaced by $\overline{d}_2$. Let us define these BCB curves as $\psi_{(ML)(LR^2LR)^m}$.

The related *lower boundaries* are associated with the family of periodicity regions of the second level between the 3-cycle and the 5-cycle, which accumulate on the 5-cycle, having horizontal boundaries colliding with d_2, and associated with cycles of symbolic sequence $(RLR)(LR^2LR)^{m-1}$, thus let $\overline{R} = (RLR)(LR^2LR)^{m-1}$. The added step is with the fixed upper boundary of the 4-cycle, that is, ψ_{MLLR}, a collision with d_2 from M side, say $\overline{L} = (MLLR)$. Then we apply the first adding step to get $\overline{R}\overline{L}$ i.e. $(RLR)(LR^2LR)^{m-1}(MLLR)$ for the lower boundaries. We have so obtained the BCB curves

$$\psi_{(ML)(LR^2LR)^m}, \quad \psi_{(RLR)(LR^2LR)^{m-1}(MLLR)} \tag{92}$$

completing the quadrilateral regions on the right of Π_7 [see also Fig. 11(b)].

In order to show that our assumption of the existence of intersection points which are not visible is realistic, we consider a different section of the parameter space, in which the assumption in (90) for $m = 1$ is evidenced, showing an intersection between the two BCB curves ψ_{MLLR} (a collision with $\overline{d}_2$ from M side) and ψ_{RLR} (a collision with $\overline{d}_2$ from R side). We have considered the (a_M, μ_R) plane keeping fixed $d_1 = 1.7$ and the other parameters as before, that is, $a_L = 0.9, a_R = 0.4$, $\mu_L = 1$, $\mu_M = 0.2, \overline{d}_2 = 1.8$, as reported in Fig. 12.

In Fig. 12(a) we can see the same bifurcation points as P_2^* and S_2^*, which may be considered similar to P_2 and S_2 of our previous figures, and Fig. 12(b) shows the enlarged portion of interest, which includes the value $a_M = 0.3$ used in the previous figures [vertical line in Fig. 12(b)]. Here, in Fig. 12(b), we can see that the periodicity region Π_7 of the 7-cycle, as well as the other regions that we shall consider below, are issued from a big bang bifurcation point P^* which cannot be seen in the section (d_2, μ_R) used before. It follows that in this section, the two BCB curves ψ_{MLLR} and ψ_{RLR} (representing a collision with d_2 from the left and right sides, respectively) are intersecting at the point P^* and we have the proper conditions to apply the adding scheme.

Besides the families of regions located on the left and on the right of the region Π_7, there exist also families of periodicity regions located above and below the region Π_7 (see Fig. 11). To determine the upper and lower boundaries of these regions, we consider that these intersect somewhere in the parameter space, as shown at the point P^* in Fig. 12(b), so that we can apply the adding scheme.

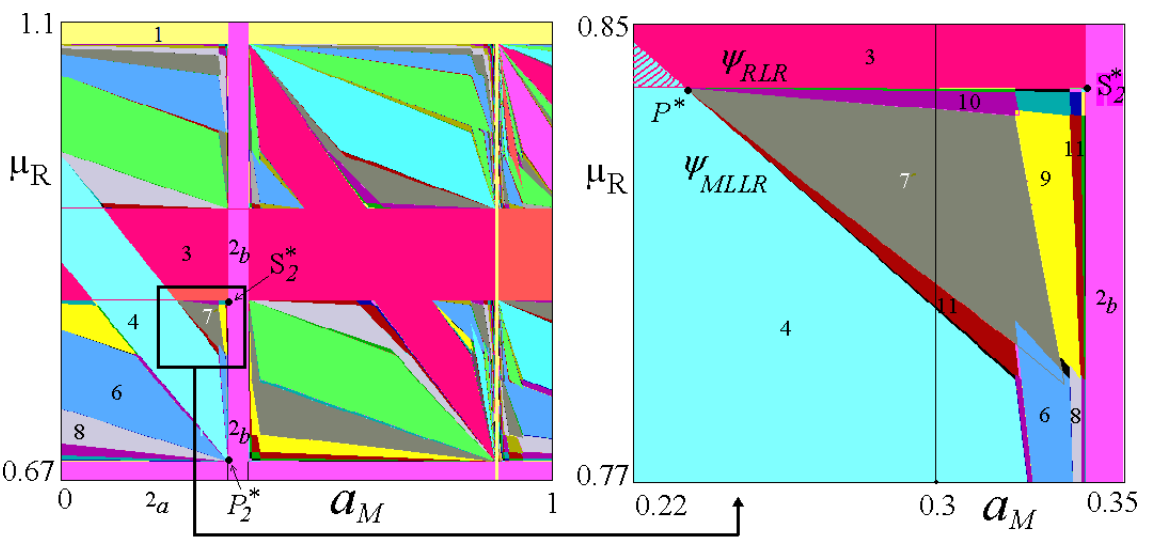

(a) (b)

Fig. 12. Two-dimensional bifurcation diagram in the (a_M, μ_R) parameter plane at $a_L = 0.9, a_R = 0.4, \mu_L = 1, \mu_M = 0.2$, $d_1 = 1.7, \overline{d}_2 = 1.8$.

Consider the BCB curves ψ_{RLR} (thus say $\overline{R} = RLR$) and the BCB curve ψ_{MLLR} (say $\overline{L} = MLLR$). Then for the first family, above Π_7, accumulating on $\overline{R}$, we consider the BCB curves associated with the symbolic sequence $\overline{L}\overline{R}^m$ and $\overline{R}\overline{L}\overline{R}^{m-1}$ which, after substitution, give

$$\psi_{(MLLR)(RLR)^m}, \quad \psi_{(RLR)(MLLR)(RLR)^{m-1}}. \tag{93}$$

In this way, we obtain the horizontal boundaries of the family (of first complexity level) of the periodicity regions located above Π_7. For the family of periodicity regions located below Π_7 accumulating on $\overline{L}$, i.e. the BCB curve ψ_{MLLR}, the horizontal boundaries are given by the BCB curves associated with the symbolic sequence $\overline{L}\overline{R}\overline{L}^{m-1}$ and $\overline{R}\overline{L}^m$, that is:

$$\psi_{(MLLR)(RLR)(MLLR)^{m-1}}, \quad \psi_{(RLR)(MLLR)^m} \tag{94}$$

As one can easily see, for both families, the horizontal boundaries of the region Π_7 represent the special case for $m = 1$.

So far we have determined the horizontal boundaries of the two families of periodicity regions located below and above Π_7. Clearly, the remaining two boundaries of each of these regions are given by the BCB curves associated with collisions of periodic points (of the same cycles) with the discontinuity d_1. To determine the BCB on the left and right sides of the *upper family*, we consider that (as before for the family having limit set on the line $d_2 = \overline{d}_2$) the family of second level $\phi_{(LR^2LR)(RLR)^{m-1}}$ (collision from the L side with d_1, say $\overline{L} = (LR^2LR)(RLR)^{m-1}$) accumulating on the BCB ψ_{RLR} of the 3-cycle is involved together with the BCB curve ϕ_{ML} (collision from the M side with d_1, say $\overline{R} = ML$), then adding $\overline{L}\overline{R} = (LR^2LR)(RLR)^{m-1}(ML) = LR(RLR)^m ML$ gives the lateral BCB on the left side while adding $\overline{R}\overline{L} = (ML)(LR^2LR)(RLR)^{m-1} = (MLLR)(RLR)^m$ gives the lateral BCB curve on the right side, thus we obtain the BCB curves:

$$\begin{aligned} \phi_{(LR^2LR)(RLR)^{m-1}(ML)} &= \phi_{LR(RLR)^m ML}, \\ \phi_{(ML)(LR^2LR)(RLR)^{m-1}} &= \phi_{(MLLR)(RLR)^m} \end{aligned} \tag{95}$$

completing the quadrilateral regions above Π_7 accumulating on ψ_{RLR} (the symbolic sequence is clearly a cyclic sequence of those in (93)) [see also Fig. 11(a)].

To determine the lateral boundaries of the BCB curves of the *lower family*, below Π_7, consider the family of periodicity regions of the cycles having symbolic sequence $(MLLR)^{m-1}(ML)$ accumulating on the boundary of the 4-cycle, colliding with d_1 from the right, defining $\overline{R} = (MLLR)^{m-1}(ML)$ and the boundary of the 5-cycle colliding with d_1 from the left, defining $\overline{L} = (LR^2LR)$, then adding $\overline{L}\overline{R} = (LR^2LR)(MLLR)^{m-1}(ML)$ gives the lateral BCB curve on the left while adding $\overline{R}\overline{L} = (MLLR)^{m-1}(ML)(LR^2LR) = (MLLR)^m(RLR)$ gives the lateral BCB on the right, thus we obtain the BCB curves:

$$\phi_{(LR^2LR)(MLLR)^{m-1}(ML)}, \phi_{(MLLR)^m(RLR)} \tag{96}$$

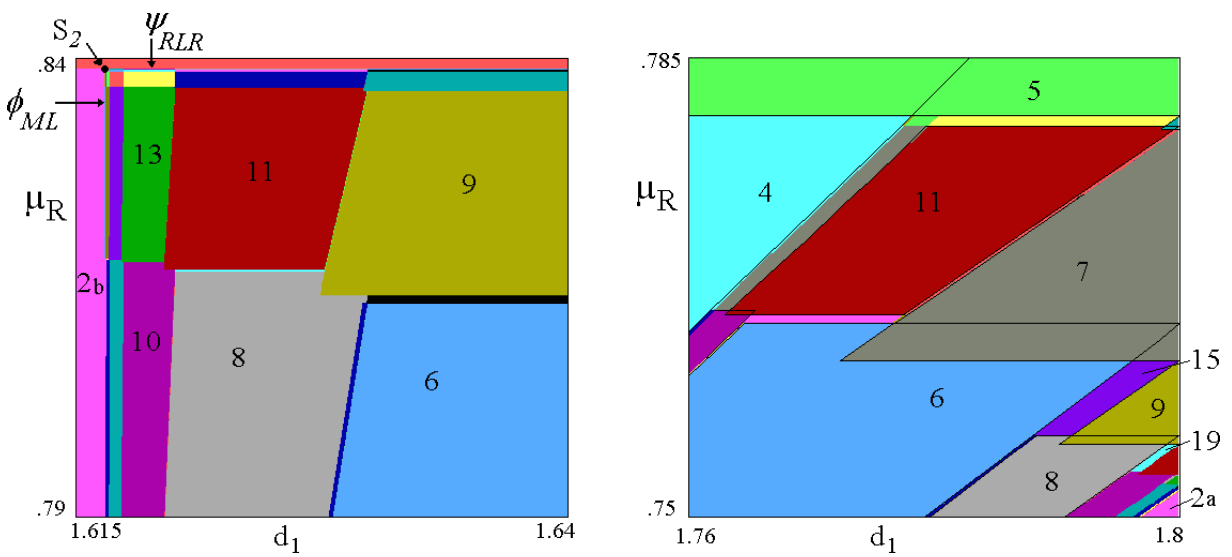

(a) (b)

Fig. 13. (a) Enlargement of the white rectangle in Fig. 11(a). (b) Enlargement of the white rectangle in Fig. 11(b).

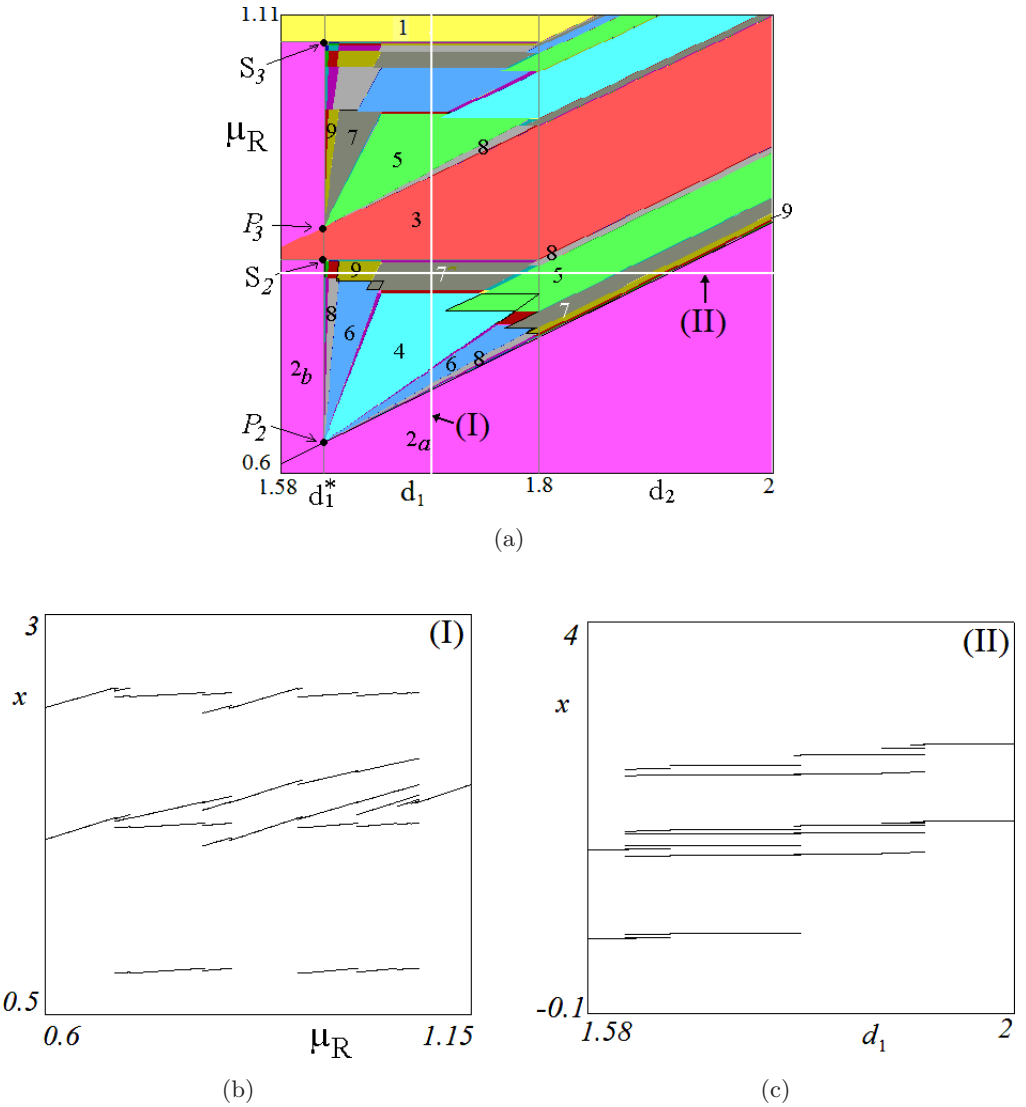

(a)

(b)

(c)

Fig. 14. (a) Two-dimensional bifurcation diagram of the map T in the parameter plane (d_1, μ_R) as in Fig. 1(b). Along the paths at (I) $d_1 = 1.7$, and (II) $\mu_R = 0.824$, the one-dimensional bifurcation diagram is reported in (b) and (c), respectively.

completing the quadrilateral regions below Π_7 accumulating on ψ_{MLLR} (the symbolic sequence is clearly a cyclic sequence of those in (94)) [see also Fig. 11(b)].

Let us return to a few comments associated with Fig. 11. As always in the period adding structure, all the quadrilateral regions so obtained are disjoint from each other and disjoint from the periodicity regions whose border is involved in the adding scheme for the quadrilateral regions. We have described above a first level of complexity, with one index only $m \geq 1$, but clearly all levels of complexity exist. Moreover, each quadrilateral region has two corners which are overlapped with other periodicity regions, thus leading, each overlapping, to two points having the same properties of points S_2 and S_3. See the enlargements in Fig. 13.

We end the present section showing in Fig. 14 examples of one-dimensional bifurcation diagrams representing the state variable x as a function of one parameter only, along the paths (I) and (II) of Fig. 14(a). Although it is not observable, infinitely many periodicity regions are crossed.

5. Conclusions

In this work, we have investigated the border collision bifurcation (BCB) curves occurring in a one-dimensional piecewise linear map with two

discontinuities, in the case of slopes all positive and less 1. We have demonstrated that the period-adding structures, known to occur in the case of maps with one point of discontinuity, also occur in the case of maps with many discontinuities, and may be formed in this case by orbits containing periodic points located in more than two partitions. In Sec. 2 we have recalled and reformulated in a suitable way the adding mechanism for a map with only one discontinuity. In Sec. 3 we have proved that independent of the number of partitions of the map, an intersection of two BCB curves associated with cycles colliding with the same point of discontinuity leads to an organizing center in the parameter space (big bang bifurcation point), from which infinitely many BCB curves are issued. The symbolic sequences of the cycles emerging at this point can be calculated using the usual Farey-tree like sequence adding scheme. Hereby the sequences of the cycles simultaneously undergoing the BCBs at the big bang bifurcation point act as the starting sequences for the adding scheme. Moreover, we have shown that the Leonov's method for the calculation of bifurcation curves in piecewise linear maps is applicable independently of the number of partitions of the investigated map, and due to the linearity of the components of our map, all the presented results are analytically obtained.

In Sec. 4 we have applied the adding mechanism described in Sec. 3 to determine several families of BCB curves of the map under study. This mechanism has been used both for the description of periodicity regions of triangular shape and of quadrilateral shape. As whichever is the chosen section of the eight-dimensional parameter space, a periodicity region of a map with two discontinuity points can have at most four BCB curves.

An open problem in the investigation of piecewise smooth maps defined on many partitions regards the situation where the BCB curves of two cycles intersect, but the cycles undergoing the BCBs collide at different points of discontinuity (as the points S_2 and S_3 and infinitely many others). The question whether it is possible to predict the structure of the parameter space close to these points remains for further studies. In the particular example considered in this work we have demonstrated that such points can be seen as bifurcation points of a special type, representing limit sets of a doubly infinite sequence of periodicity regions (and thus BCB curves).

To conclude, we remark that Theorem 1 proved in this work can also be applied to piecewise linear maps with many partitions (more than two discontinuities), the only assumption is that two different stable cycles collide with the same discontinuity point.

The dynamic behavior of our map T when the slopes satisfy different conditions is a problem left for further studies.

References

Avrutin, V. & Schanz, M. [2006] "On multi-parametric bifurcations in a scalar piecewise-linear map," *Nonlinearity* **19**, 531–552.

Avrutin, V., Schanz, M. & Banerjee, S. [2006] "Multi-parametric bifurcations in a piecewise-linear discontinuous map," *Nonlinearity* **19**, 1875–1906.

Avrutin, V., Schanz, M. & Gardini, L. [2010] "Calculation of bifurcation curves by map replacement," *Int. J. Bifurcation and Chaos* **20**, 3105–3135.

Banerjee, S., Karthik, M. S., Yuan, G. & Yorke, J. A. [2000a] "Bifurcations in one-dimensional piecewise smooth maps — theory and applications in switching circuits," *IEEE Trans. Circuits Syst.-I: Fund. Th. Appl.* **47**, 389–394.

Banerjee, S., Ranjan, P. & Grebogi, C. [2000b] "Bifurcations in two-dimensional piecewise smooth maps — theory and applications in switching circuits," *IEEE Trans. Circuits Syst.-I: Fund. Th. Appl.* **47**, 633–643.

Banerjee, S. & Grebogi, C. [1999] "Border-collision bifurcations in two-dimensional piecewise smooth maps," *Phys. Rev. E* **59**, 4052–4061.

Bischi, G. I. & Merlone, U. [2009] "Global dynamics in binary choice models with social influence," *J. Math. Sociol.* **33**, 1–26.

Bischi, G. I., Gardini, L. & Merlone, U. [2009] "Periodic cycles and bifurcation curves for one-dimensional maps with two discontinuities," *J. Dyn. Syst. Geomet. Th.* **7**, 101–123.

Bischi, G. I., Gardini, L. & Tramontana F. [2010] "Bifurcation curves in discontinuous maps," *Discr. Contin. Dyn. Syst. B* **13**, 249–267.

Day, R. [1982] "Irregular growth cycles," *Amer. Econ. Rev.* **72**, 406–414.

Day, R. [1994] *Complex Economic Dynamics* (MIT Press, Cambridge).

di Bernardo, M., Feigin, M. I., Hogan, S. J. & Homer, M. E. [1999] "Local analysis of C-bifurcations in n-dimensional piecewise smooth dynamical systems," *Chaos Solit. Fract.* **10**, 1881–1908.

Feely, O., Fournier-Prunaret, D., Taralova-Roux, I. & Fitzgerald, D. [2000] "Nonlinear dynamics of bandpass sigma-delta modulation. An investigation

by means of the critical lines tool," *Int. J. Bifurcation and Chaos* **10**, 303–327.

Fournier-Prunaret, D., Feely, O. & Taralova-Roux, I. [2001] "Lowpass sigma-delta modulation: An analysis by means of the critical lines tool," *Nonlin. Anal.* **47**, 5343–5355.

Gallegati, M., Gardini, L., Puu, T. & Sushko, I. [2003] "Hicks' trade cycle revisited: Cycles and bifurcations," *Math. Comput. Simul.* **63**, 505–527.

Gardini, L., Puu, T. & Sushko, I. [2006a] "The Hicksian model with investment floor and income ceiling," *Business Cycles Dynamics. Models and Tools*, eds. Puu, T. & Sushko, I. (Springer-Verlag, NY), pp. 179–191.

Gardini, L., Puu, T. & Sushko, I. [2006b] "A Goodwin-type model with a piecewise linear investment function," *Business Cycles Dynamics. Models and Tools*, eds. Puu, T. & Sushko, I. (Springer-Verlag, NY), pp. 317–333.

Gardini, L., Sushko, I. & Naimzada, A. K. [2008] "Growing through chaotic intervals," *J. Econ. Th.* **143**, 541–557.

Gardini, L. & Tramontana, F. [2010] "Border collision bifurcations in 1D PWL map with one discontinuity and negative jump. Use of the first return map," *Int. J. Bifurcation and Chaos* **20**, 3529–3135.

Gardini, L., Tramontana, F., Avrutin, V. & Schanz, M. [2010] "Border collision bifurcations in 1D PWL map and Leonov's approach," *Int. J. Bifurcation and Chaos* **20**, 3085–3104.

Gardini, L., Merlone, U. & Tramontana, F. [2011] "Inertia in binary choices: Continuity breaking and big-bang bifurcation points," *J. Econ. Behav. Organiz.* **80**, 153–167.

Halse, C., Homer, M. & di Bernardo, M. [2003] "C-bifurcations and period-adding in one-dimensional piecewise-smooth maps," *Chaos Solit. Fract.* **18**, 953–976.

Hao, B.-L. [1989] *Elementary Symbolic Dynamics and Chaos in Dissipative Systems* (World Scientific, Singapore).

Hommes, C. H. [1991] *Chaotic Dynamics in Economic Models*, Ph.D. Thesis (Wolters-Noodhoff, Groningen).

Hommes, C. H. & Nusse, H. [1991] "Period three to period two bifurcations for piecewise linear models," *J. Econ.* **54**, 157–169.

Hommes, C. H. [1995] "A reconsideration of Hick's nonlinear trade cycle model," *Struct. Change. Econ. Dyn.* **6**, 435–459.

Hommes, C. H., Nusse, H. & Simonovits, A. [1995] "Cycles and chaos in a socialist economy," *J. Econ. Dyn. Cont.* **19**, 155–179.

Keener, J. P. [1980] "Chaotic behavior in piecewise continuous difference equations," *Trans. Amer. Math. Soc.* **261**, 589–604.

Leonov, N. N. [1959] "On a pointwise mapping of a line into itself," *Radiofisisica* **2**, 942–956.

Leonov, N. N. [1962] "On a discontinuous pointwise mapping of a line into itself," *Dolk. Acad. Nauk SSSR* **143**, 1038–1041.

Maistrenko, Y. L., Maistrenko, V. L. & Chua, L. O. [1993] "Cycles of chaotic intervals in a time-delayed Chua's circuit," *Int. J. Bifurcation and Chaos* **3**, 1557–1572.

Maistrenko, Y. L., Maistrenko, V. L., Vikul, S. I. & Chua, L. O. [1995] "Bifurcations of attracting cycles from time-delayed Chua's circuit," *Int. J. Bifurcation and Chaos* **5**, 653–671.

Maistrenko, Y. L., Maistrenko, V. L. & Vikul, S. I. [1998] "On period-adding sequences of attracting cycles in piecewise linear maps," *Chaos Solit. Fract.* **9**, 67–75.

Mira, C. [1987] *Chaotic Dynamics* (World Scientific, Singapore).

Nusse, H. E. & Yorke, J. A. [1992] "Border-collision bifurcations including period two to period three for piecewise smooth systems," *Physica D* **57**, 39–57.

Nusse, H. E. & Yorke, J. A. [1995] "Border-collision bifurcations for piecewise smooth one-dimensional maps," *Int. J. Bifurcation and Chaos* **5**, 189–207.

Puu, T., L. Gardini & Sushko, I. [2002] "Cournot duopoly with kinked linear demand according to Palander and Wald," *Oligopoly and Complex Dynamics: Tools and Models*, eds. Puu, T. & Sushko, I. (Springer–Verlag, NY).

Puu, T. & Sushko, I. [2002] *Oligopoly Dynamics, Models and Tools* (Springer-Verlag, NY).

Puu, T., Gardini, L. & Sushko, I. [2005] "A Hicksian multiplier-accelerator model with floor determined by capital stock," *J. Econ. Behav. Organ.* **56**, 331–348.

Puu, T. & Sushko, I. [2006] *Business Cycle Dynamics, Models and Tools* (Springer Verlag, NY).

Puu, T. [2007] "The Hicksian trade cycle with floor and ceiling dependent on capital stock," *J. Econ. Dyn. Cont.* **31**, 575–592.

Schelling, T. C. [1973] "Hockey helmets, concealed weapons and daylight saving," *J. Confl. Resol.* **17**, 381–428.

Schelling, T. C. [1978] *Micromotives and Macrobehavior* (W.W. Norton, NY).

Sushko, I., Puu, T. & Gardini, L. [2003] "The Hicksian floor-roof model for two regions linked by interregional trade," *Chaos Solit. Fract.* **18**, 593–612.

Sushko, I., Gardini, L. & Puu, T. [2004] "Tongues of periodicity in a family of two-dimensional discontinuous maps of real Möbius type," *Chaos Solit. Fract.* **21**, 403–412.

Sushko, I., Agliari, A. & Gardini, L. [2005] "Bistability and border-collision bifurcations for a family of

unimodal piecewise smooth maps," *Discr. Contin. Dyn. Syst.–Series B* **5**, 881–897.

Sushko, I., Agliari, A. & Gardini, L. [2006] "Bifurcation structure of parameter plane for a family of unimodal piecewise smooth maps: Border-collision bifurcation curves," *Chaos Solit. Fract.* **29**, 756–770.

Tramontana, F., Gardini, L. & Puu, T. [2009] "Duopoly games with alternative technologies," *J. Econ. Dyn. Cont.* **33**, 250–265.

Zhusubaliyev, Z. T. & Mosekilde, E. [2003] *Bifurcations and Chaos in Piecewise-Smooth Dynamical Systems* (World Scientific, Singapore).

Zhusubaliyev, Z. T., Mosekilde, E., Maity, S., Mohanan, S. & Banerjee, S. [2006] "Border collision route to quasiperiodicity: Numerical investigation and experimental confirmation," *Chaos* **16**, 023122, 1–11.

Zhusubaliyev, Z. T., Soukhoterin, E. & Mosekilde, E. [2007] "Quasiperiodicity and torus breakdown in a power electronic dc/dc converter," *Math. Comput. Simul.* **73**, 364–377.